MARTIN MARIETTA ENERGY SYSTEMS LIBRARIES
3 4456 0361445 3

143

CENTRAL RESEARCH LIBRARY
DOCUMENT COLLECTION

ORNL-2869
UC-81 - Reactors-Power

THERMAL AND RESONANCE ABSORPTION CROSS SECTIONS OF THE U^{233}, U^{235}, AND Pu^{239} FISSION PRODUCTS

E. A. Nephew

CENTRAL RESEARCH LIBRARY
DOCUMENT COLLECTION
LIBRARY LOAN COPY
DO NOT TRANSFER TO ANOTHER PERSON
If you wish someone else to see this document, send in name with document and the library will arrange a loan.

OAK RIDGE NATIONAL LABORATORY
operated by
UNION CARBIDE CORPORATION
for the
U.S. ATOMIC ENERGY COMMISSION

Printed in USA. Price $1.50. Available from the

Office of Technical Services
Department of Commerce
Washington 25, D.C.

LEGAL NOTICE

This report was prepared as an account of Government sponsored work. Neither the United States, nor the Commission, nor any person acting on behalf of the Commission:

A. Makes any warranty or representation, expressed or implied, with respect to the accuracy, completeness, or usefulness of the information contained in this report, or that the use of any information, apparatus, method, or process disclosed in this report may not infringe privately owned rights; or

B. Assumes any liabilities with respect to the use of, or for damages resulting from the use of any information, apparatus, method, or process disclosed in this report.

As used in the above, "person acting on behalf of the Commission" includes any employee or contractor of the Commission, or employee of such contractor, to the extent that such employee or contractor of the Commission, or employee of such contractor prepares, disseminates, or provides access to, any information pursuant to his employment or contract with the Commission, or his employment with such contractor.

ORNL-2869

Reactors—Power
TID-4500 (15th ed.)

Contract No. W-7405-eng-26

REACTOR PROJECTS DIVISION

THERMAL AND RESONANCE ABSORPTION CROSS SECTIONS OF THE U^{233}, U^{235}, AND Pu^{239} FISSION PRODUCTS

E. A. Nephew

DATE ISSUED

JAN 18 1960

OAK RIDGE NATIONAL LABORATORY
Oak Ridge, Tennessee
operated by
UNION CARBIDE CORPORATION
for the
U. S. ATOMIC ENERGY COMMISSION

MARTIN MARIETTA ENERGY SYSTEMS LIBRARIES

3 4456 0361445 3

TABLE OF CONTENTS

Symbols and Definitions iv

Abstract 1

Introduction 1

Stable and Long-Lived Fission Products 3

High-Cross-Section Fission Products 6
Low-Cross-Section Fission Products 6

Composition of the Fission Product Aggregate as a Function of the Fractional Burnup and Flux Spectrum 8

Burnout Equations 8
Calculation of the Saturation Index, α 11

Fission Product Data 14

Resonance Data on Major Components of Fission Product Aggregate 14
Resonance Integral of the Fission Products Above 100 ev 18

Effect of Reactor Specific Power and Neutron Temperature on the Fission Product Aggregate Cross Section 18

Reactor Specific Power 18
Neutron Temperature 19

Psuedoelements 23

Results of Calculations 25

Appendix 1. Reactor Spectra and Effective Cross Sections 39

Appendix 2. Calculation of the Resonance Absorption Integral 41

References 44

Bibliography 46

SYMBOLS AND DEFINITIONS

I_T = total excess over 1/v resonance integral from μKT ev to 10^6 ev

Σ_μ = total resonance absorption integral of the fission product above μKT including the 1/v part

Σ_f = total fission integral of the fuel including the 1/v part

σ_f = fission cross section of the fuel at 2200 m/sec

T = neutron temperature in degrees Kelvin

K = Boltzman's constant

μKT = the low energy cutoff of the 1/E flux ($\mu = 5$)

$$\alpha_i = \frac{\hat{\sigma}_i}{\hat{\sigma}_f} = (1 - P)\frac{g\sigma_0}{g_f\sigma_f} + P\frac{\Sigma_\mu}{\Sigma_f} \text{ (saturation index)}$$

P = the percent of fissions due to the epithermal or 1/E flux

$$g = \frac{\int_0^\infty \sigma(v)\, v\, n(v)\, dv}{\sigma_0 v_0 \int_0^\infty n(v)\, dv}$$

$I_{<100}$ = the excess resonance absorption integral below 100 ev

$I_{>100}$ = the excess resonance absorption integral above 100 ev

$I_T = I_{<100} + I_{>100}$

σ_0 = 2200 m/sec absorption cross section

β = spectral index specifying the degree of flux thermalization

v_0 = 2200 meters/sec

y_i = the fission yield of the fuel for fission product i

λ_i = the radioactive decay constant of the fission product

$F = \int \hat{\sigma}_f\, \phi(t)\, dt$, the fractional burnup of the fuel

$\hat{\sigma}_i$ = the effective cross section for a 2200 m/sec flux

ϕ = the "2200 m/sec flux"

R = the reactor specific power in kw/kg of fissionable material

THERMAL AND RESONANCE ABSORPTION CROSS SECTIONS OF THE U^{233}, U^{235}, AND Pu^{239} FISSION PRODUCTS

Abstract

The absorption cross section of the fission product aggregate of U^{233}, U^{235}, and Pu^{239} has been calculated as a function of irradiation and the degree of flux thermalization. Especial attention has been given to the resonance integral of the fission products in the range of 0 to 100 ev. The saturation characteristics of the individual fission products which in turn determine the composition of the fission product aggregate are calculated for fluxes with different epithermal contents. The parameter P used to specify the degree of flux thermalization represents the fraction of fissions due to the neutrons in the 1/E portion of the flux. By summing over the individual fission products, a resulting thermal cross section and an energy distributed resonance integral have been obtained for the fission product aggregate of the three fuels as a function of P and F. Here, F is the fractional burnup of the fuel, defined as $F = \int \hat{\sigma}_f \, \phi(t) \, dt$. For F = 0 and T = 1000°K, the effective thermal cross sections are calculated to be 37, 43, and 54 barns per fission for U^{233}, U^{235}, and Pu^{239}, respectively. At the same conditions, the excess resonance integrals below 100 ev are calculated to be 134, 172, and 266 barns per fission for U^{233}, U^{235}, and Pu^{239}, respectively.

By grouping the individual fission products which have similar saturation characteristics, it has been possible to designate four pseudoelements which when taken together yield the same total thermal cross section and resonance integral as that of the fission product aggregate over the range of P and F values considered. Multigroup cross sections have been computed and are listed for each pseudoelement for use in a 32-group code. Thermal group cross sections are also listed for each pseudoelement for neutron temperatures between 69 and 2704°F.

Introduction

During the operation of a reactor, fission products consisting of a large number of both stable and unstable nuclei are formed and accumulate. In general, these nuclei capture neutrons and compete with the fuel nuclei as neutron sinks. As a result the criticality constant and

breeding ratio of the reactor decrease and the reactor becomes poisoned. A quantitative knowledge of all the fission product cross sections as a function of energy is needed in order to make realistic predictions of reactor behavior. For convenience we use the term fission product aggregate to refer to all the fission products as a group, excluding Xe^{135} and a Sm^{149} composite group, which are treated separately. It is important to note that the composition and hence the absorption characteristics of the fission product aggregate are functions of both the fractional fuel burnup and the degree of flux thermalization. In this study we have chosen the parameter P to represent the degree of flux thermalization, where P is the fraction of total fissions due to the epithermal flux content.

In a U^{235}-fueled reactor the poisoning effects of U^{236} should be considered in addition to the normal fission products. In most reactors, U^{236} cannot be regarded as a fertile material, since U^{237} decays with a 6.75-day half life to form nonfissionable Np^{237}. It would require a flux of more than 2×10^{15} neutrons/cm^2·sec to cause appreciable fission in U^{237} before it decays. In this study, the properties of the fission product aggregate have been investigated both with and without the inclusion of U^{236} as a fission product. The effects of U^{236} impose a severe additional strain upon the prospects of low resonance reactors. The importance of absorptions in the resonance region has been emphasized by Weinberg and Wigner (1), who state: "The fission product poisoning in the low resonance region is so great that such reactors would require frequent reprocessing. There is serious doubt whether a low resonance reactor can operate long enough without reprocessing to make power production in the low resonance region economically feasible."

The composition of the fission product aggregate arrives at a steady-state condition only when all the individual components have reached saturation. This condition corresponds to very high irradiation times and is never actually attained. Of more immediate interest is to know how the composition and thus the absorption cross section of the fission product aggregate varies with fuel burnup and its dependence upon the flux level and epithermal content.

In nuclear fission more than 80 primary products are formed, most of which undergo several stages of radioactive decay and transformation by neutron capture before being converted into stable nuclei. Consequently there are over 200 isotopes of 30 or more different elements present among the fission products after a short time. To treat each mass chain explicitly and in full detail is not possible because of incomplete physical data. Usually, the thermal cross section, the direct yield, and the resonance integral data are not known for all the members of a given mass chain. In addition, radioactive nuclides complicate the calculations by introducing an additional independent variable. Fortunately, in most cases it is only the stable end product and its immediate parent that remain in the reactor long enough to capture a significant number of neutrons.

From the above considerations, it is evident that suitable restrictions must be applied in order to simplify the problem. Therefore, we make the assumption that the stable end product in a given mass chain is produced directly from fission. This is convenient, since few cross sections of unstable nuclides are known and since the growth equations of a nuclide become much more tractable if the time dependency is removed. The assumption is equivalent to grouping the nuclides according to their half lives. Nuclides with short half lives are regarded as decaying instantaneously, whereas nuclides with long half lives are regarded as stable.

Stable and Long-Lived Fission Products

A complete tabulation of the stable and long-lived fission products and their thermal cross sections and yields is given in Table 1. Large variations are observed in both the fission yields and the thermal cross sections of the individual nuclides. A consideration of the different saturation characteristics of the fission products leads naturally to a grouping of the nuclides according to the magnitude of their absorption cross sections. Seven fission products are known to have absorption cross sections above about 10,000 barns, whereas the rest are below about

Table 1. Stable and Long-Lived Fission Products

Fission Product	σ_0 (barns)	Y (%)			Included in Calculations*
		U^{235}	U^{233}	Pu^{239}	
Ge^{72}	0.94	1.6×10^{-5}		0.0012	a
Ge^{73}		1.1×10^{-4}			a
Ge^{74}		3×10^{-4}			c
As^{75}		8×10^{-4}			a
Ge^{76}		0.015			a
Se^{77}	0.42	0.0083	0.019		a
Se^{78}	0.4 ± 0.4	0.021			a
Se^{79} (6×10^4 y)		0.056			a
Se^{80}	0.03	0.08			b, c
Br^{81}	3.1	0.14			c, d
Se^{82}	2	0.25			a, d
Kr^{83}	220 ± 40	0.544	1.14	0.29	Yes
Kr^{84}	0.10	1.00	1.90	0.47	a
Rb^{85}	0.80	1.30	0.56		a, d
Kr^{85} (10.3 y)	<15	0.293	0.56	0.55	a, d
Kr^{86}	0.06 ± 0.02	2.02	3.18	0.75	a, d
Rb^{87} (6×10^{10} y)	0.12 ± 0.03	2.49			a, d
Sr^{88}	0.005 ± 0.001	3.57	5.30	1.39	d
Y^{89}	1.31 ± 0.08	4.79	6.5	1.9	Yes
Sr^{90} (28 y)	1.0 ± 0.6	5.77	5.80	2.31	Yes
Zr^{91}	1.58 ± 0.12	5.84	6.53		Yes
Zr^{92}	0.25 ± 0.12	6.03	6.70		d
Zr^{93}	<4	6.45	7.10		Yes
Zr^{94}	9.08 ± 0.06	6.40	6.82		d
Mo^{95}	13.9 ± 0.14	6.27	6.10		Yes
Zr^{96}	0.10 ± 0.10	6.33	5.60		d
Mo^{97}	2.2 ± 0.7	6.09	5.35		Yes
Mo^{98}	0.40 ± 0.40	5.78	5.18		Yes
Tc^{99} (2.1×10^5 y)	22 ± 3	6.06	4.8	5.9	Yes
Mo^{100}	0.50 ± 0.50	6.30	4.40		d
Ru^{101}	2.46	5.00	3.00		Yes
Ru^{102}	1.44 ± 0.16	4.1	2.37		a, d
Rh^{103}	156 ± 7	3.0	1.6	5.8	Yes
Ru^{104}	0.7 ± 0.2	1.8	0.96		a, d
Pd^{105}		0.90		3.9	c, d
Ru^{106} (1.01 y)		0.38	0.28	5.0	c, d
Pd^{106}		0.38	0.28	5.0	c, d
Pd^{107} (7×10^6 y)		0.19			c, d
Pd^{108}	10 ± 2	0.08			c, d
Ag^{109}	87 ± 7	0.03	0.04	1.5	a, d
Pd^{110}	0.30 ± 0.10	0.02			a, d
Cd^{111}		0.019	0.025	0.27	c
Cd^{112}	0.03 ± 0.015	0.01	0.016	0.10	
Cd^{113}	20,000	0.01			Yes (Table 2)
Cd^{114}	1.1 ± 0.14	0.01			a
In^{115} (6×10^{14} y)	207	0.0104	0.020	0.041	Yes
Cd^{116}	1.5 ± 0.3	0.01			a
Sn^{117}		0.01			c
Sn^{118}	0.01	0.01			a
Sn^{120}	0.001	0.01			a
Sb^{121}	5.9 ± 0.5	0.015			a

*Notations a, b, c, and d indicate that the fission product is not included in the calculations because (a) $y\sigma_0 < 0.02$, (b) y unknown, (c) σ_0 unknown, (d) resonance data unknown.

Table 1 (continued)

Fission Product	σ_0 (barns)	Y (%)			Included in Calculations*
		U^{235}	U^{233}	Pu^{239}	
Sm^{122}	0.16	0.013			a
Sb^{123}	4.1 ± 0.3	0.0013			a
Sm^{124}					b, c
Sb^{125} (2 y)		0.021	0.05	0.072	c, d
Te^{125}	1.56 ± 0.16	0.021			a, d
Te^{126}	0.80 ± 20	0.05			a
I^{127}	7 ± 0.6	0.250		0.39	Yes
Te^{128}	0.30 ± 0.30	0.37			a, d
I^{129} (1.7×10^7 y)	11 ± 0.4	0.90		5.5×10^{-4}	Yes
Te^{130}	0.5 ± 0.3	2.0			a, d
Xe^{131}	120 ± 15	2.93	3.74	2.87	Yes
Xe^{132}	0.2 ± 0.1	4.38	5.10	4.02	a, d
Cs^{133}	29 ± 1	6.59	6.18	5.27	Yes
Xe^{134}	0.2 ± 0.1	8.06	6.54	5.69	Yes
Xe^{135} (9.2 hr)	$(2.72 \pm 0.11) \cdot 10^6$	6.30	6.00	7.27	Yes (Table 2)
Cs^{135} (2.6×10^6 y)	13 ± 0.4	6.41	>4.9	5.53	
Xe^{136}	0.15 ± 0.08	6.46	<8.9	5.06	a, d
Cs^{137} (29 y)	<2	6.15	7.16	5.24	Yes
Ba^{138}	0.7 ± 0.1	5.74		6.26	d
La^{139}	8.2 ± 0.8	6.55	5.91	5.7	Yes
Ce^{140}	0.66 ± 0.06	6.44	5.6	5.68	d
Pr^{141}	11.6 ± 0.6	6.00	5.57	5.2	Yes
Ce^{142}	1.0 ± 0.2	5.95	5.60	6.69	d
Nd^{143}	324 ± 10	5.98	5.20	6.31	Yes
Ce^{144} (285 d)		~6.0	4.1	5.29	c, d
Nd^{144} (5×10^{15} y)	5 ± 0.6	5.67	4.0	5.29	Yes
Nd^{145}	60 ± 6	3.95	3.0	4.24	Yes
Nd^{146}	10 ± 1	3.07	2.3	3.53	Yes
Pm^{147} (2.65 y)	60 ± 20	2.70	1.71	2.92	Yes
Sm^{147} (1.3×10^{11} y)	87 ± 60	2.38	1.71	2.92	No
Nd^{148}	3.4 ± 1	1.70	1.15	2.28	d
Sm^{149}	40,800 ± 900	1.13	0.61	1.89	Yes (Table 2)
Nd^{150}	3.0 ± 1.5	0.67	0.48	1.38	d
Sm^{151} (80 y)	10,000 ± 2,000	0.45	0.26	1.17	Yes
Sm^{152}	224 ± 7	0.285	0.17	0.83	Yes
Eu^{153}	450 ± 20	0.150	0.095	0.41	Yes
Sm^{154}	5.5 ± 1.1	0.077	0.037	0.32	a, d
Eu^{155} (1.9 y)	14,000 ± 4,000	0.03		0.22	Yes (Table 2)
Gd^{155}	61,000 ± 5,000	0.03		0.22	Yes (Table 2)
Gd^{156}		0.014		0.12	c, d
Gd^{157}	240,000 ± 12,000	0.0078			Yes (Table 2)
Gd^{158}	4 ± 2	0.002			a
Tb^{159}	46 ± 4	0.00107			a
Gd^{160}	0.8 ± 3	0.0003			a
U^{236}	5.5	0.19			Yes

*Notations a, b, c, and d indicate that the fission product is not included in the calculations because (a) $y\sigma_0 < 0.02$, (b) y unknown, (c) σ_0 unknown, (d) resonance data unknown.

500 barns. Equilibrium between product and removal rates is reached at much lower irradiation times for the first group than for the second. Consequently, nuclides belonging to the high-cross-section group quickly reach their maximum number density in the reactor, while the number

density of those belonging to the low-cross-section group increases nearly linearly with irradiation for a large range of F values. For small irradiations only the first group need be considered, but for longer irradiations the second group becomes increasingly important.

High-Cross-Section Fission Products

Poisoning calculations for the high-cross-section fission products are usually carried out by treating Xe^{135} and Sm^{149} explicitly and separately. If desired, the remaining nuclides can be lumped with Sm^{149}. In this case, the total yield for the samarium group is 1.66% and the effective thermal cross section is 33,088 barns. Data on these high-cross-section fission products are included in Table 2.

Table 2. High-Cross-Section Fission Products

Fission Product	Half Life	σ_0 (barns)	y for U^{235} (%)	$y\sigma_0$ (barns per fission)
Xe^{135}	9.2 h	2.72×10^6	6.3	1.714×10^5
Sm^{149}	Stable	40,800	1.13	461.04
Sm^{151}	80 y	10,000	0.45	45.00
Gd^{155}	Stable	61,000	0.03	18.30
Eu^{155}	1.9 y	14,000	0.03	4.20
Cd^{113}	Stable	20,000	0.01	2.00
Gd^{157}	Stable	240,000	0.0078	18.72

Low-Cross-Section Fission Products

The remainder of this study is concerned only with the absorption characteristics of the low-cross-section fission products. As used in this report, the term fission product aggregate refers only to the low-cross-section fission products. The nuclides which are considered as important contributors to the thermal and resonance cross sections of the fission product aggregates of U^{233}, U^{235}, and Pu^{239} are listed in Table 3.

Table 3. Thermal Cross Sections of the Low-Cross-Section Fission Products at a Neutron Temperature of 1000°K

Fission Product	$y g \sigma_0$		
	U^{233}	U^{235}	Pu^{239}
Nd^{143}	15.888	18.270	19.279
Rh^{103}	3.075	5.765	11.147
Xe^{131}	4.488	3.515	3.444
Nd^{145}	1.803	2.665	2.523
Cs^{133}	1.792	1.910	1.528
Sm^{152}	0.870	1.485	4.045
Pm^{147}	1.026	1.427	1.752
Te^{99}	1.063	1.341	1.307
Kr^{83}	2.508	1.196	0.638
U^{236}		1.044	
Sm^{150}	0.519	0.960	1.607
Mo^{95}	0.848	0.871	0.872
Pr^{141}	0.646	0.695	0.698
Eu^{153}	0.372	0.586	1.603
La^{139}	0.485	0.536	0.467
Nd^{146}	0.230	0.306	0.353
Nd^{144}	0.200	0.283	0.265
Zr^{93}	0.284	0.257	0.258
I^{129}	0.243	0.242	0
Mo^{97}	0.118	0.133	0.134
Ru^{101}	0.074	0.122	0.123
Cs^{137}	0.143	0.122	0.105
Zr^{91}	0.103	0.091	0.092
Y^{89}	0.085	0.062	0.025
Sr^{90}	0.058	0.057	0.023
Ag^{109}	0.035	0.025	1.305
Mo^{98}	0.021	0.022	0.023
In^{115}	0.049	0.025	0.101
Xe^{134}		0.015	
I^{127}	0.018	0.017	0.027
Aggregate	37.044	44.045	53.744

Composition of the Fission Product Aggregate as a Function of Fractional Burnup and Flux Spectrum

Burnout Equations

At a given fractional burnup, F, there are i different isotopes present in the fission product aggregate, each characterized by its individual relative abundance, absorption cross section, and cumulative fission yield. That is, at F, there are present in the reactor:

N_1 nuclei of isotope 1, absorption cross section $\hat{\sigma}_1$, yield y_1
N_2 nuclei of isotope 2, absorption cross section $\hat{\sigma}_2$, yield y_2
.. ..
N_i nuclei of isotope i, absorption cross section $\hat{\sigma}_i$, yield y_i

The growth rate of a particular isotope is the difference between the production and removal rates. Thus, for isotope i

$$\frac{dN_i}{dt} = y_i \hat{\sigma}_f N_f \, \phi(t) - \hat{\sigma}_i N_i \, \phi(t) - \lambda_i N_i \quad , \tag{1}$$

where $\phi(t)$ is the "2200 m/sec flux" and $\hat{\sigma}_i$ is the effective cross section consistent with this convention of neutron flux (see Appendix 1). For simplification we assume continuous fuel replenishment, that is, N_f remains constant. The change of variables $F = \int \hat{\sigma}_f \, \phi(t) \, dt$ aids the analysis since the flux may be time dependent. This new independent variable designates accumulative fissions per original fuel atom or per cent of fuel burnup. Because of the assumption of continuous fuel replenishment, F is not limited to unity but may increase without limit. The differential equation becomes

$$\frac{dN_i}{dF} = y_i N_f - \alpha_i N_i \quad , \tag{2}$$

where

$$\alpha_i = \frac{\hat{\sigma}_i}{\hat{\sigma}_f} + \frac{\lambda}{\hat{\sigma}_f \phi} \quad ,$$

whose solution, subject to the conditions $N_i = 0$ at $F = 0$, is

$$N_i = y_i N_f \frac{1 - e^{-\alpha_i F}}{\alpha_i} \quad . \tag{3}$$

Equation 3 represents the total number of nuclei of isotope i present in the reactor at any irradiation time F. Dividing this number by the total number of fission product pairs which have been formed up to time F and multiplying by the effective absorption cross section, $\hat{\sigma}_i$, gives the contribution of isotope i in barns per fission to the total cross section of the fission product aggregate, which is indicated by the subscript fpa,

$$\hat{\sigma}^i_{fpa} = \hat{\sigma}_i y_i \frac{1 - e^{-\alpha_i F}}{\alpha_i F} \quad . \tag{4}$$

The effective cross section of the fission product aggregate is obtained by summing the contributions over all of the fission products.

$$\hat{\sigma}_{fpa} = \sum_{i=1}^{n} \hat{\sigma}_i y_i \frac{1 - e^{-\alpha_i F}}{\alpha_i F} \quad . \tag{5}$$

A specific fission product with a given absorption property, either thermal cross section or resonance integral, contributes that property to the fission product aggregate in an amount dependent upon the relative concentration of the specific fission product to the fission product aggregate as a whole. Thus, the given absorption property is multiplied by two weighting factors, the first weighting factor being the cumulative yield of the isotope and the second weighting factor being an expression of the tendency of the particular isotope to saturate. Inspection of the second weighting factor,

$$\frac{1 - e^{-\alpha_i F}}{\alpha_i F} \quad ,$$

shows that if $\alpha F \rightarrow 0$, the weighting factor approaches 1, whereas, if $\alpha F \rightarrow \infty$, the weighting factor approaches zero. Qualitatively this expresses the fact that fission products with large absorption cross sections, hence large α's, saturate quickly, and their relative contribution to the aggregate cross section decreases with increasing F. Fission products with small absorption cross sections, hence small α's, continue to build up with F, and their relative contributions to the aggregate cross section increase in magnitude.

Equation 5 gives the contribution to the aggregate cross section by a given mass chain due to first-order effects only. It is tacitly implied that the new product formed by neutron capture has a nonappreciable absorption cross section and contributes nothing to the over-all fission product properties. If such is not the case, second-order effects must also be calculated. Consider the reaction in which a nuclide N_2 is formed by neutron capture in N_1; $\hat{\sigma}_1$ and y_1 are the cross section and yield associated with N_1 and $\hat{\sigma}_2$ is the cross section associated with N_2 ($\hat{\sigma}_2 \neq 0$). The differential equation governing the growth of the second-order poison is

$$\frac{dN_2}{dt} = \hat{\sigma}_1 N_1 \, \phi(t) - \hat{\sigma}_2 N_2 \, \phi(t) = y\hat{\sigma}_f N_f \, \phi(t) \left[1 - e^{-\hat{\sigma}_1 \phi(t)}\right] - \hat{\sigma}_2 N_2 \, \phi(t)$$

or

$$\frac{dN_2}{dF} = yN_f \left[1 - e^{-(\hat{\sigma}_1/\hat{\sigma}_f)F}\right] - \frac{\hat{\sigma}_2}{\hat{\sigma}_f} N_2 \quad . \tag{6}$$

Solving Eq. 6 subject to the boundary conditions $N_2 = 0$ when $F = 0$, gives for the number of N_2 nuclei present in the reactor at time F,

$$N_2 = yN_f \frac{\hat{\sigma}_f}{\hat{\sigma}_2} \left[1 - \frac{\hat{\sigma}_2}{\hat{\sigma}_2 - \hat{\sigma}_1} e^{-(\hat{\sigma}_1/\hat{\sigma}_f)F} + \frac{\hat{\sigma}_1}{\hat{\sigma}_2 - \hat{\sigma}_1} e^{-(\hat{\sigma}_2/\hat{\sigma}_f)F}\right] \quad . \tag{7}$$

The contribution of the given mass chain to the over-all fission product cross section is then

$$\sigma_{fpa}(A) = y_A \hat{\sigma}_1 \left[\frac{1 - e^{-(\hat{\sigma}_1/\hat{\sigma}_f)F}}{\frac{\hat{\sigma}_1}{\hat{\sigma}_f} F} \right] +$$

$$+ y_A \hat{\sigma}_2 \left[\frac{1 - \frac{\hat{\sigma}_2}{\hat{\sigma}_2 - \hat{\sigma}_1} e^{-(\hat{\sigma}_1/\hat{\sigma}_f)F} + \frac{\hat{\sigma}_1}{\hat{\sigma}_2 - \hat{\sigma}_1} e^{-(\hat{\sigma}_2/\hat{\sigma}_f)F}}{\frac{\hat{\sigma}_2}{\hat{\sigma}_f} F} \right] . \qquad (8)$$

It is noted that in this formulation the second-order contribution from mass chain A may come from the same nuclide which is formed directly from fission in mass chain A + 1. That is, the calculations may repeatedly include the same nuclide with different ancestry. The analysis is readily extended to include third and higher order effects. Actual quantitative estimates, however, are difficult to obtain because of the paucity of complete absorption cross section data for a given chain. Consequently, with the single exception of mass chain 151, the calculations made in this study include only first-order effects. This fact, together with the possible existence of nuclides with important absorption cross sections at present unknown, imposes the nature of a lower limit on the results reached in this report. It may be mentioned here that Sampson et al. (2) in their study of fission product thermal cross sections estimate that higher order effects become appreciable above $F = 1$ and contribute 20% or more to the total thermal cross section at $F = 3$.

Calculation of the Saturation Index, α

In Eq. 5 the exponential term specifying the effective absorption cross section of a nuclide is defined as

$$\alpha_1 = \frac{\hat{\sigma}_i}{\hat{\sigma}_f} + \frac{\lambda}{\hat{\sigma}_f \phi} \quad ,$$

that is, the ratio of the absorption rate to the fission rate. It is assumed, after Westcott (3) (see Appendix 1), that the reactor flux spectrum can be represented by a Maxwellian distribution together with a slowing down 1/E tail cut off at μKT. The flux here is a function only of energy, with no time or spatial dependence taken into account. For a stable nuclide with absorption cross section $\sigma(E)$, the reaction rate per nucleus is given by

$$\sigma_i \phi_{2200} = (n\bar{v})_M \int_0^\infty \sigma(E) \frac{E}{(KT)^2} e^{-E/KT} dE + (n\bar{v})_M \beta \int_{\mu KT}^\infty \sigma(E) \frac{dE}{E}$$

$$= (n\bar{v})_M \left[\left(\frac{\pi T_0}{4T} \right)^{1/2} g\sigma_0 + \beta \Sigma_\mu \right] \quad . \tag{9}$$

The ratio of the absorption rate to the fission rate defines α_i as

if $\beta = 0$

$$\alpha_i = \frac{\hat{\sigma}_i \phi_{2200}}{\hat{\sigma}_f \phi_{2200}} = \frac{(n\bar{v})_M \left[\left(\frac{\pi T_0}{4T} \right)^{1/2} g\sigma_0 + \beta \Sigma_\mu \right]}{(n\bar{v})_M \left[\left(\frac{\pi T_0}{4T} \right)^{1/2} g_f \sigma_f + \beta \Sigma_f \right]} \quad . \tag{10}$$

If we denote by P the fraction of total fissions which are due to the epithermal or 1/E part of the flux, then

$$\alpha_i = \frac{g_i \sigma_i}{g_f \sigma_f} \times \frac{1}{1+P} + \frac{P}{1+P} \times \frac{\Sigma_\mu}{\Sigma_f}$$

$$P = \frac{\beta \Sigma_f}{\left(\frac{\pi T_0}{4T}\right)^{1/2} g_f \sigma_f}$$

if $P \ll 1$ then

$$\alpha_i = (1 - P) \frac{g\sigma_0}{g_f \sigma_f} + P \frac{\Sigma_\mu}{\Sigma_f} \quad . \tag{11}$$

The second term in the above expression allows for absorptions in the resonance region due to 1/E neutrons. For nuclides with large resonance

integrals this term may be predominant in determining α_i for reasonable values of P. This means that absorptions in the resonance region can play a significant role in determining how quickly a given nuclide saturates. If the neutron flux has an appreciable epithermal content, serious underestimates of fission product poisoning will result if resonance absorptions are neglected. This is clearly illustrated in Fig. 1, where the ratio of absorptions in the U^{235} fission product aggregate to the absorptions which would occur if the aggregate cross section followed a strict 1/v energy dependence is plotted versus the fraction of total fissions due to thermal absorptions in the fuel.

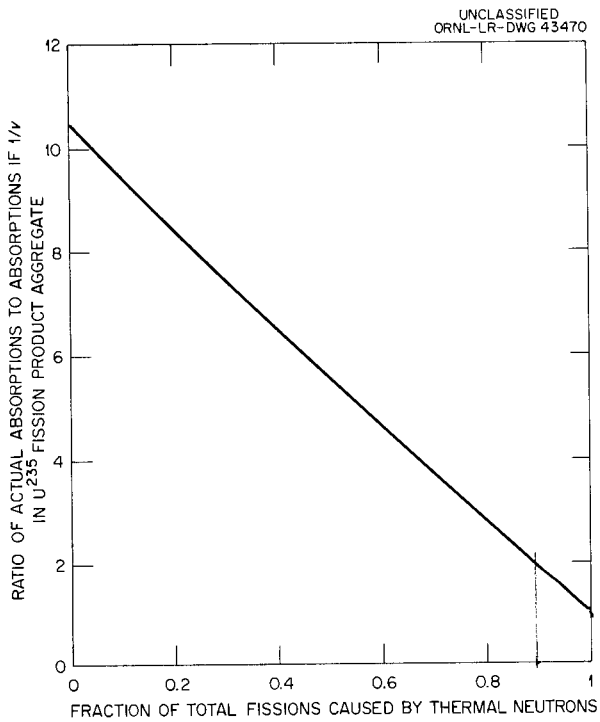

Fig. 1. Deviation of the U^{235} Fission Product Aggregate Cross Section From the 1/v Law for Different Neutron Fluxes.

The following fuel constants, taken from ref 3, have been used in calculating α at a neutron temperature of 1000°K:

	U^{233}	U^{235}	Pu^{239}
g_f	1.0376	0.912	2.4613
σ_f	527 barns	580 barns	746 barns
Σ_f	805 barns	271 ± 25 barns	319 barns

Fission Product Data

The stable and long-lived fission products which are considered to constitute the fission product aggregate were listed in Table 3 above. The cumulative fission yields for each nuclide were taken from the compilation by Katcoff (4), and the thermal cross sections were taken from BNL-325, 2nd ed. (5). The excess resonance absorption integrals used in the calculations are listed in Table 4, together with values from other compilations. In most cases the resonance integrals were derived from the resonance parameters in BNL-325, 2nd ed., using Eqs. A.7 and A.8 of Appendix 2. The uncertainties associated with these derived values amount to about 20 or 30% because of uncertainties in the resonance parameters and resonance energies alone. This fact, together with the large spread of values reported in the literature, indicates that an experimental program aimed at definitely establishing the resonance integrals of the more important fission products would be well justified. In addition to undertaking a systematic search for the possible existence of other high-yield, high-resonance-integral fission products, emphasis should also be given to reducing the uncertainties associated with the resonance integrals of the first 12 nuclides of Table 4. In fission-product poisoning studies, reliable fission yields are equally important, and in this respect much still remains to be desired, especially in the cases of U^{233} and Pu^{239}. In this study the fission yields for these two nuclides were obtained mainly from the Katcoff (4) compilation and from a report by Pattenden (6). Where the yields are not known, the U^{235} fission yield is assumed.

Resonance Data on Major Components of Fission Product Aggregate

Data for the more important contributors to the resonance features of the fission product aggregate are given below. The symbol I_T denotes the total absorption resonance integral in excess over 1/v, whereas Σ_μ

Table 4. Excess Resonance Integrals of the Low-Cross-Section Fission Products

Fission Product	Excess Resonance Integral Below 100 ev, $I_{<100}$ (barns)	Total Excess Resonance Integral, I_T (barns)	Source Reference	I_T (barns) from Other Compilations Given for Comparison (reference number is in parentheses)
U^{236}	256	256 ± 22	7	295*
Pm^{147}	1950	2050 ± 400	8	~2000 (6)
Rh^{103}	980	1000 ± 20	11	600 (6), 656 (9),** 529 (10)**
Cs^{133}	345.2	375 ± 71	*	450 (6), 490 ± 80 (14), 320 (13)
Xe^{131}	687.7	768 ± 170	*	690 (6)
Sm^{152}	2850	2850 ± 300	14	1960 (6), 2850 ± 300 (14), > 1750 (9)**
Tc^{99}	108.2	168 ± 20	*	170 (6), 60 ± 20 (14), 106 (15)
Nd^{145}	243.5	310 ± 60	*	350 (6), 130 ± 15 (14)
Mo^{95}	96.4	101 ± 15	*	100 (6), 100 ± 20 (14)
Ru^{101}	116.8	131 ± 131	*	
Eu^{153}	1121	1512 ± 880	*	1800 (6), 1280 ± 100 (14), 950 (9)**
Nd^{143}	13.5	37.4 ± 2.2	*	15 (6), <50 (14)
La^{139}	8.66	24.7 ± 1.5	*	
Ag^{109}	1358	1396 ± 60	*	1160 (9),** 1870 ± 200 (14), 1174 (10)**
Mo^{97}	6.60	12.2 ± 2	*	13.8 (15), 19 ± 2.5 (14)
In^{115}	3166	3202 ± 90	*	3500 (12), 3600 ± 350 (14), 2640 (9)**
I^{127}	117	167 ± 20	*	140 (9),** 180 ± 30 (14), 116 (10)**
Pr^{141}	2.4	16 ± 8	*	11.3 (9),** 5.3 (10)**
I^{129}	6.4	25 ± 1	*	36 ± 4 (7)

*Calculated from parameters in BNL-325, 2nd ed., from equations (4), (5) Appendix 2.

**The values listed from references 9 and 10 are measured activation resonance integrals, not excess resonance integrals.

denotes the total resonance absorption integral above μKT including the 1/v part. With $\mu = 5$ and $T = 1000°K$ the low energy integration limit is nearly equal to the cadmium cutoff energy.

U^{236}. A measured resonance capture integral of $\Sigma_\mu = 257 \pm 22$ barns and a thermal cross section of 5.5 ± 0.3 barns is reported in ref 7. An excess resonance integral of $I_{<100} = 256$ barns is used in this study.

Pm^{147}. From the resonance parameters listed in ref 8, an excess resonance integral below 100 ev of $I_{<100} = 1950 \pm 400$ is calculated. The higher energy contribution based on the statistical model is estimated to be ~100 barns. The values used in this study are $I_{<100} = 1950$ barns, $I_T = 2050$ barns.

Rh^{103}. An excess resonance integral below 100 ev of $I_{<100} = 1007 \pm 17$ barns is calculated from the parameters in ref 5. A higher energy contribution of about 17 barns is estimated from the statistical model. Macklin and Pomerance (9) report a measured value of $\Sigma_\mu = 656$ barns based on the activation method. Other values reported are $I_T = 600$ barns (ref 6), $\Sigma_\mu = 529$ barns (ref 10), and $I_T = 980$ barns (ref 11).

Nearly all the resonance integral of Rh^{103} arises from the large resonance at 1.257 ev. Experimental determinations of the resonance integral are therefore very sensitive to the self-shielding factor assumed in evaluating the results. Since fission products in a reactor more closely approach the condition of infinite dilution with no self-shielding, it was decided to use the value of 980 barns, which is nearly the result calculated from the parameters. The values used in this study are $I_{<100} = 980$ barns, $I_T = 1024$ barns.

Cs^{133}. From the parameters listed in ref 5, an excess resonance integral below 100 ev of $I_{<100} = 345 \pm 71$ barns is calculated. Higher energy contributions are estimated to be ~30 barns. Other values reported in the literature are $I_T = 450$ barns (ref 6), $I_T = 420$ barns (ref 12), $I_T = 320$ barns (ref 13). In addition, a measured value of $I_T = 490 \pm 80$ barns obtained by the pile oscillator technique is reported in ref 14. This paper appeared after nearly all the calculations in

this study were completed. It is felt that the resonance integrals listed in ref 14 may represent the latest and best determinations. The values used in this study are $I_{<100}$ = 345.2 barns, I_T = 375 barns.

Xe^{131}. An excess resonance integral below 100 ev of $I_{<100}$ = 688 ± 170 barns is calculated from the parameters listed in ref 5. Higher energy contributions are estimated as ~80 barns. The values used in this study are $I_{<100}$ = 688 barns, I_T = 765 barns.

Sm^{152}. No resonance parameters are listed in ref 5. Values reported in the literature are Σ_μ > 1750 barns (ref 9), Σ_μ = 1790 barns (ref 15) and Σ_μ = 1504 barns (ref 10). In addition, a measured value of I_T = 2850 ± 300 barns obtained by the pile oscillator technique is reported in ref 14. The values used in this study are $I_{<100}$ = 2850 barns, I_T = 2850 barns. All the resonance integral is considered to be due to the large resonance at 8.1 ev.

Ru^{101}. Resonance parameters in ref 5 refer to the naturally occurring element. The three ruthenium fission products Ru^{101}, Ru^{102}, and Ru^{103} have U^{235} fission yields of 5, 4.1, and 1.8% and natural abundances of 17, 31.3, and 18.3%, respectively. The maximum ruthenium contribution to the excess resonance integral of the U^{235} fission product aggregate is calculated to be 11.68 barns per fission. This occurs for the case in which all the resonances are assumed to be due to Ru^{101}. If all the resonances were assigned to Ru^{102} or Ru^{103}, the contributions to the fission product resonance integral would be about 5.2 and 4 barns per fission, respectively. Since the picture is somewhat complicated by the likelihood that the odd isotopes have a closer level spacing than the even ones and since the three ruthenium isotopes in question amount to only two-thirds of the natural element, it is not possible to arrive at a definitive result. In this study, the ruthenium contribution to the fission products excess resonance integral is rather arbitrarily taken as 5.84 barns per fission.

Other Fission Products. Excess resonance integrals for the remaining fission products listed in Table 4 are calculated from the resonance parameters given in ref 5.

Resonance Integral of the Fission Products Above 100 ev

Several independent estimates (16, 17, 18) of the U^{235} fission product resonance capture cross sections have been made for the energy range from 10^2 ev to 10^6 ev. Based on these estimates, a total absorption resonance integral per pair of U^{235} fission products of the order of 20 to 25 barns is calculated. Gordeev and Pupko (18) estimate the total resonance integral of the fission product aggregate in this energy range to be 23 barns per fission, the value which is adopted in this study. Estimates of the high energy resonance integrals of the U^{233} and Pu^{239} fission product aggregate show the over-all total to be about the same as for U^{235}, in spite of variations in yield for the individual fission products. These estimates were made on the basis of data for the individual nuclides given in ref 16.

Effect of Reactor Specific Power and Neutron Temperature on the Fission Product Aggregate Cross Section

Reactor Specific Power

The inclusion of radioactive Pm^{147}, $t_{1/2} = 2.65$ y, in Table 4 as an important contributor to the properties of the fission product aggregate makes the end result dependent upon the reactor flux level as specific power. If R is the reactor specific power in kw/kg, the saturation index α of Eq. 2 becomes, in the case of U^{235} fuel,

$$\alpha_1 = \frac{\lambda_1}{\hat{\sigma}_{f\phi}} + \frac{\hat{\sigma}_1}{\hat{\sigma}_f} = \left[\frac{686}{R} + (1 - P)\frac{g\sigma_0}{g_f\sigma_f} + P\frac{\Sigma_\mu}{\Sigma_f}\right] . \qquad (12)$$

Putting in the cross section values for U^{235} and Pm^{147} at 1000°K yields

$$\alpha_1 = \left[\frac{686}{R} + 0.113 + P(7.58)\right] . \qquad (13)$$

Here it is noted that α_1 exhibits a comparatively weak dependence upon R over reasonable values of R and P. We find, for example, that for P = 0.2, R = 2000 ± 1000 kw/kg, and T = 1000°K, α_1 becomes

$$\alpha_1 = 1.973\ (1 \pm 0.20) \quad . \tag{14}$$

Properly, the decay product Sm^{147} of Pm^{147} should also be taken into account. The effect of Sm^{147} is to make the fission product aggregate still less dependent upon the flux level, since its flux dependence is opposite to that of Pm^{147}. The rate of formation of Sm^{147} is

$$\frac{dN_2}{dt} = \lambda_1 N - \hat{\sigma}_2 N_2 \phi \quad , \tag{15}$$

so

$$\frac{N_2}{FN_f} = \frac{y_1 \lambda_1}{\lambda_1 + \hat{\sigma}_1 \phi} \left(\frac{e^{-\alpha_2 F} - e^{-\alpha_1 F}}{\alpha_2 - \alpha_1} + \frac{1 - e^{-\alpha_2 F}}{\alpha_2 F} \right) \quad . \tag{16}$$

Based on a thermal cross section of 87 barns and an excess resonance integral of 495 barns for Sm^{147}, the U^{235} fission product aggregate has been calculated and plotted in Fig. 2 for different values of R. As expected, the dependency of the aggregate cross section on the reactor specific power is small. It is felt therefore that the pseudoelement cross sections (described in a subsequent section), which are calculated for a specific power of 2000 kw/kg, may be used for other R values without too great an error. It is noted here that the results shown in Fig. 2 were calculated on the basis of a U^{235} aggregate resonance integral of 166 barns. Hence the curves are to be interpreted on a qualitative basis only.

Neutron Temperature

The cross sections of most of the fission products listed in Table 3 depart from 1/v behavior for Maxwellian spectra. The Westcott g-factor

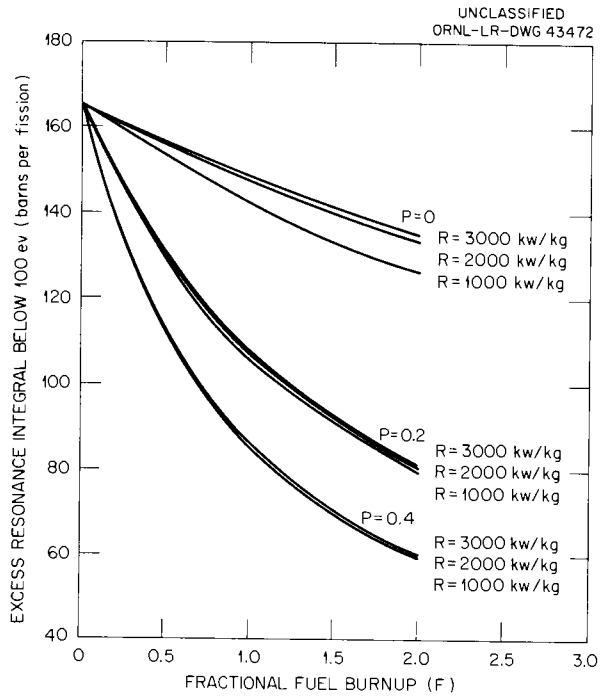

Fig. 2. Variation of the U^{235} Fission Product Aggregate with Reactor Specific Power.

(Appendix 1) specifies the degree of departure and is plotted in Fig. 3 as a function of the neutron temperature for several different fission products. The data plotted are taken from refs. 19, 20, and 21. It may be seen that the nuclides Rh^{103}, In^{115}, Eu^{153}, and Nd^{145} become increasingly non-1/v at higher neutron temperatures. Such behavior is expected, since these nuclides have strong low energy (~1 ev) resonances. Absorption cross section data in the energy range to about 10 ev are not available for the remaining nuclides in Table 3, so it was not possible to calculate g-factors for these isotopes. Since, with the exception of Pm^{147}, none of these nuclides have known resonances below about 5 ev, a g-factor of unity is assumed. The result of summing $yg\sigma_0$ over all components of the U^{235} fission product aggregate for several different neutron temperatures is shown in Fig. 4. Here, the aggregate thermal cross section as a function of temperature is also plotted for U^{233} and Pu^{239}.

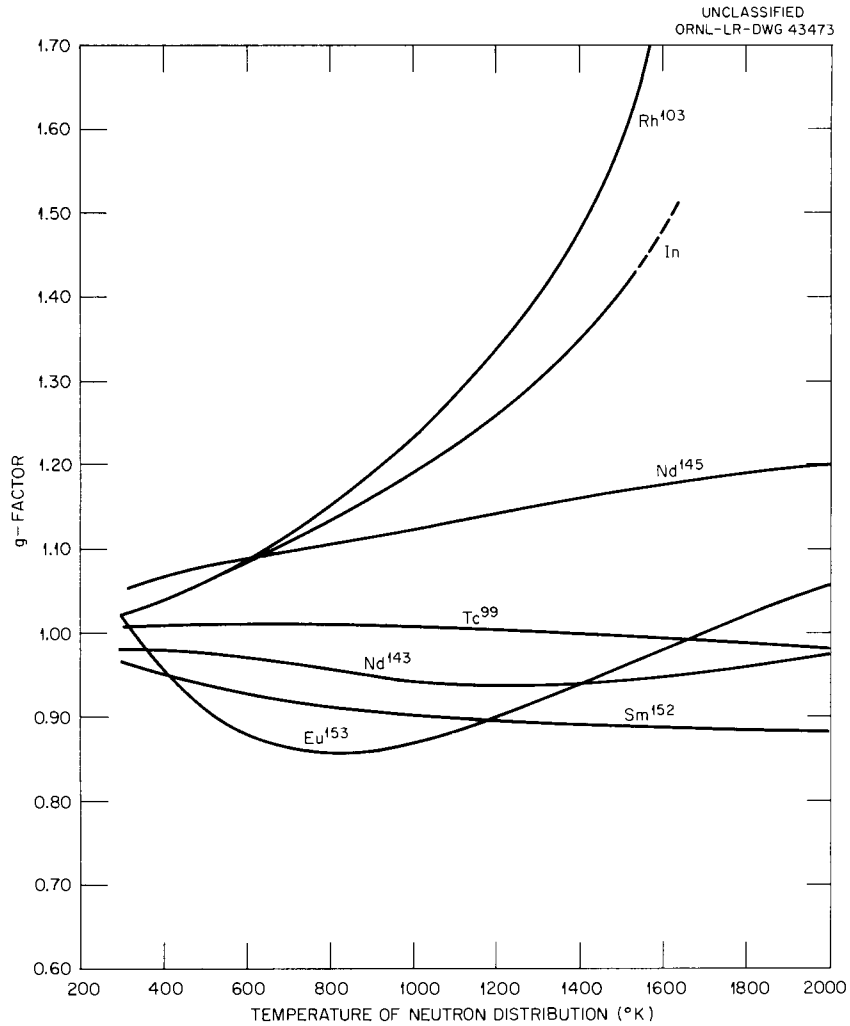

Fig. 3. Fission Product g-Factors as a Function of Neutron Temperature.

Since the effective absorption cross section of an individual fission product is a function of temperature, this means that the relative composition, and thus the absorption cross section of the fission product aggregate, is also temperature dependent. Because of this it is useful to know to what extent the pseudoelements which are derived from an assumed neutron temperature of 1000°K may be applicable at other temperatures. Calculations made for a temperature of 500°K show that the pseudoelements represent fairly well the actual fission product aggregate at this temperature. This result appears reasonable, since,

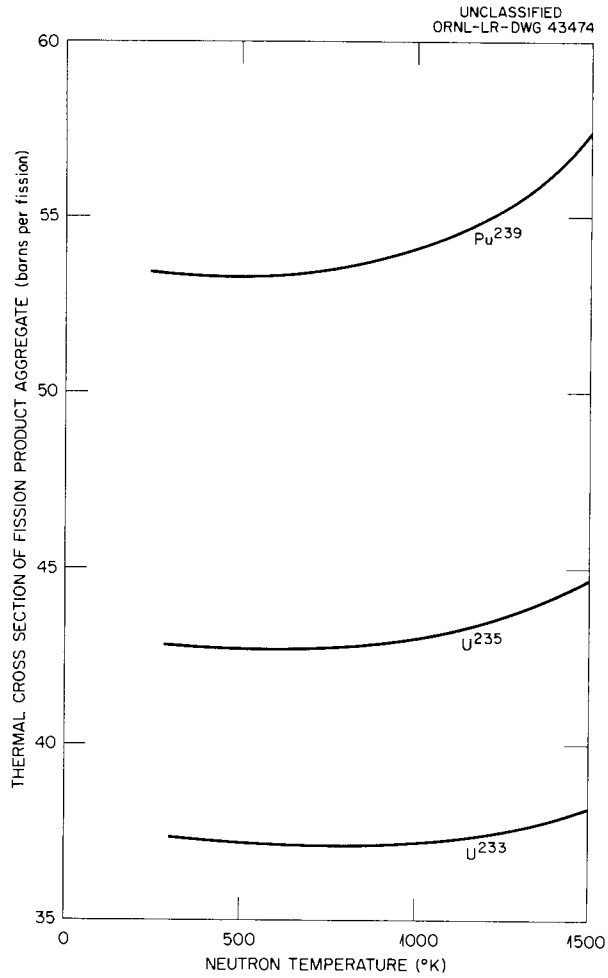

Fig. 4. Thermal Cross Section of the U^{233}, U^{235}, and Pu^{239} Fission Product Aggregate vs Neutron Temperature.

in Fig. 4, it may be seen that there is little variation in the aggregate thermal cross sections in this range of temperatures. At temperatures greater than 1000°K, it may be seen from Fig. 3 that the effective absorption cross sections of Rh^{103}, In^{115}, and Nd^{145} increase markedly and will significantly affect the composition of the fission product aggregate as a function of irradiation time. For this reason, caution must be exercised in applying the artificial pseudoelements at temperatures greater than 1000°K.

Pseudoelements

For convenience in reactor lifetime calculations it is useful to reduce the number of fission products which must be treated individually. To this end the low-cross-section fission products of Tables 1 and 2 have been assigned to four groups according to their excess resonance integrals. By determining an appropriate yield, thermal cross section, and excess resonance integral for each group as a whole, it has been possible to effectively represent the low-cross-section fission product aggregate by four pseudoelements. These pseudoelements are made up as follows:

Pseudoelement No. 1 (excess resonance integral from 0 to 100 barns)

Nd^{143}	Nd^{144}	Zr^{93}
La^{139}	Kr^{83}	Cs^{137}
Mo^{97}	Sm^{150}	Zr^{91}
I^{129}	Sr^{90}	Y^{89}
Pr^{141}	Nd^{146}	Mo^{98}
		Xe^{134}

Pseudoelement No. 2 (excess resonance integral from 100 to 500 barns)

Mo^{95}	I^{127}	U^{236}
Tc^{99}	Cs^{133}	
Ru^{101}	Nd^{145}	

Pseudoelement No. 3 (excess resonance integral from 500 to 1200 barns)

Rh^{103}	Xe^{131}

Pseudoelement No. 4 (excess resonance integral from 1200 to 3400 barns)

Ag^{109}	Sm^{152}
In^{115}	Eu^{153}
Pm^{147}	

Applying Eq. 5 to each group yields the actual variation of thermal cross section and resonance integral with P and F which is to be reproduced by the pseudoelements. In particular, the group values of $\sum_i{}' y_i \, (g\sigma_0)_i$ and $\sum_i{}' y_i \, (I_{res})_i$ which must be satisfied at F = 0 are

obtained. By trial and error an $\alpha(P)$ can be selected which best simultaneously reproduces the actual variation of $\sum_i y_i (g\sigma_0)_i$ and $\sum_i y_i \, (I_{res})_i$ over the ranges of P and F under consideration. In this study the range of P was taken from 0 to 0.4 and of F from 0 to 2. Once a group $\alpha(P)$ has been selected, the group yield is uniquely determined from the definition of $\alpha(P)$ and from the fixed values at F = 0:

$$\alpha(P)_{gr} = (1 - P) \frac{(g\sigma_0)_{gr}}{g_f \sigma_f} + P \frac{(I_{res} + c_1 g\sigma_0)_{gr}}{\Sigma_f}$$

$$(g\sigma_0)_{gr} = \frac{1}{y_{gr}} \sum_i y_i \, (g\sigma_0)_i$$

$$(I_{res})_{gr} = \frac{1}{y_{gr}} \sum_i y_i \, (I_{res})_i$$

$$y_{gr} = \frac{1}{\alpha(P)_{gr}} \left\{ (1 - P) \frac{\sum_i y_i \, (g\sigma_0)_i}{g_f \sigma_f} + P \left[\frac{\sum_i y_i \, (I_{res})_i + c_1 (g\sigma_0)}{\Sigma_f} \right] \right\} .$$

In determining the pseudoelement cross sections and yields, judgment must be excercised as to whether the thermal cross section or resonance features are the most important. For example, pseudoelement No. 1 is primarily a contributor to the thermal cross section alone, therefore an $\alpha(P)$ has been selected to best reproduce the thermal cross section variation with F. In the remaining groups, a compromise between the two properties is necessary. Furthermore, less emphasis has been placed on reproducing the burnup characteristics for P = 0 than for higher P values.

The thermal cross sections and the resonance integrals for the four pseudoelements, as determined from the above considerations, are given in Tables 11, 12, and 13 of the following section on "Results of Calculations."

Results of the Calculations

The excess resonance integral of the U^{235} fission product aggregate at zero burnup is given in Table 5. Values taken from ref 18 are included for comparison. The aggregate resonance integral is given both for the case where U^{236} is considered as a fission product and for the case it is not. The energy distribution of the excess resonance integral is shown in Table 6.

The excess resonance integral of the U^{233} and Pu^{239} fission product aggregates at F = 0 are given in Table 7. The energy-distributed resonance integrals of the fission product aggregate of these two nuclides, together with that of U^{235}, are plotted in Fig. 5. The importance of U^{236} is clearly seen here.

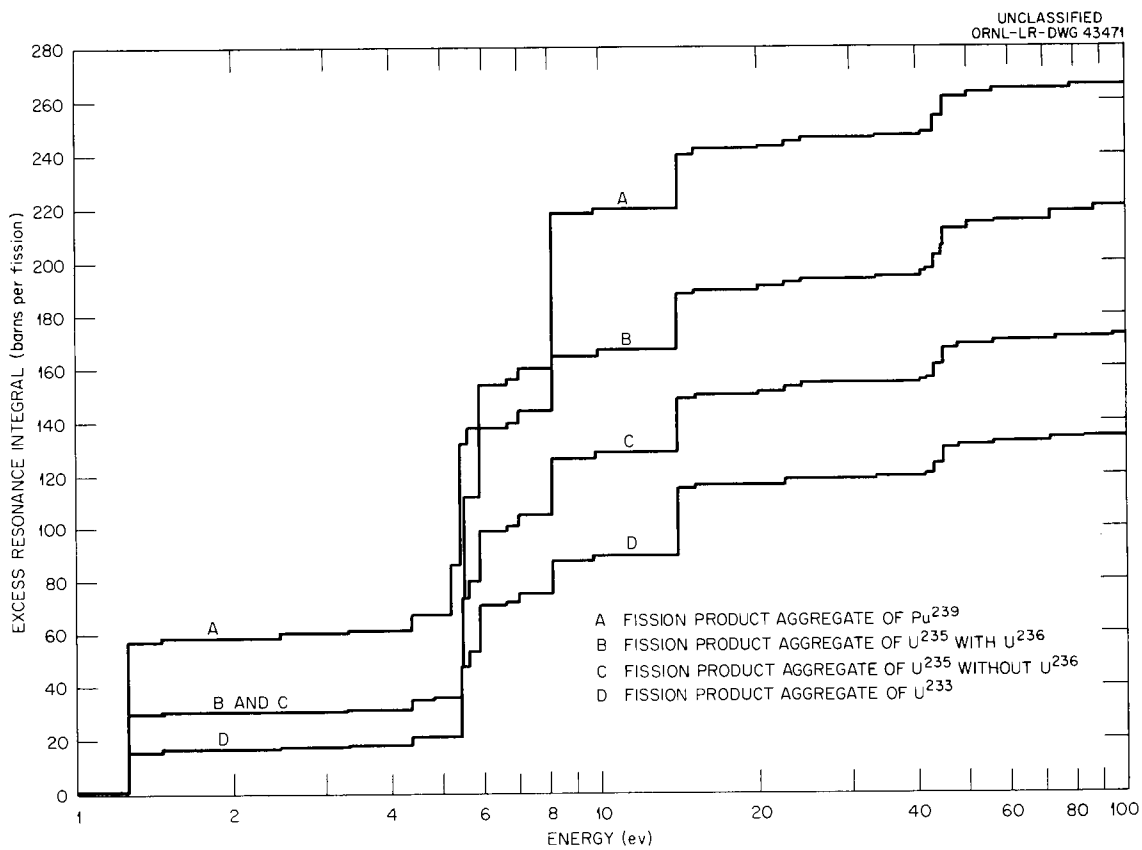

Fig. 5. Cumulative Excess Resonance Integral of the Fission Product Aggregate as a Function of Energy.

Table 5. U^{235} Fission Product Excess Resonance Integrals in the Energy Range 0–100 ev Compared with Values from Gordeev and Pupko (ref 18)

Fission Product	Values from Gordeev and Pupko (ref 18)			Values from This Paper and Katcoff (ref 4)		
	y (%) for U^{235}	$I_{<100}$ (barns)	y $I_{<100}$ (barns per fission)	y (%) for U^{235} (ref 4)	$I_{<100}$ (barns)	y $I_{<100}$ (barns per fission)
U^{236}				19.0	256	48.64
Pm^{147}	2.26	1283	29	2.38	1950	46.40
Rh^{103}	2.41	975.1	23.5	3.00	980	29.40
Cs^{133}	6.70	475.7	31.87	6.59	345.2	22.75
Xe^{131}	2.85	364.9	10.40	2.93	687.7	20.15
Sm^{152}	0.791	2300	18.20	0.735	2850	20.95
Tc^{99}	6.16	110.6	6.81	6.06	108.2	6.56
Nd^{145}	3.95	258.2	10.20	3.95	243.5	9.62
Mo^{95}	6.61	95.3	6.30	6.27	96.4	6.04
Ru^{101}	4.60	223.9	10.30	5.00	116.8	5.84
Eu^{153}	0.122	1177	1.44	0.15	1121	1.68
Nd^{143}	5.90	13.7	0.808	5.98	13.5	0.81
La^{139}	6.59	1.21	0.080	6.55	8.66	0.57
Ag^{109}	0.028	34.6	0.010	0.03	1358	0.41
Mo^{97}	6.56	6.4	0.420	6.09	6.60	0.40
In^{115}	0.011	3091	0.340	0.0104	3166	0.33
I^{127}	0.38	75.8	0.288	0.25	117	0.29
Pr^{141}	6.41	2.0	0.128	6.0	2.4	0.14
I^{129}				0.90	6.4	0.06
Xe^{133}			21.40	Not included because of short half life		
Gd^{155}	0.055	690.9	0.38	Included in Table 2		
Pd^{108}	0.13	253.1	0.33	Resonance data not available		
Pd^{105}	0.92	17.4	0.16	Resonance data not available		
Total			172.364	With U^{236}		221.04
				Without U^{236}		172.40
				$I_{>100}$		23

Table 6. Energy Distributed Excess Resonance Integral of the U^{235} Fission Product Aggregate with Gordeev and Pupko (ref 18) Values Included for Comparison

Fission Product	E_0 (ev)	yI_{res} (barns per fission)		$\sum_i y_i I_{res}$ (barns per fission)	Fission Product	E_0 (ev)	yI_{res} (barns per fission)		$\sum_i y_i I_{res}$ (barns per fission)
		From (ref 18)	This Paper				From (ref 18)	This Paper	
Cs^{133}	128		0.455	221.04	Mo^{95}	45	6.30	6.044	212.117
I^{129}	95.6		0.002	220.585	U^{236}	44.5		4.010	206.073
Rh^{103}	95.0		0.027	220.583	Pm^{147}	43.2		0.187	202.063
Cs^{133}	94.8	0.250	0.243	220.556	Nd^{145}	43.1	4.870	4.832	201.876
I^{127}	91	0.022	0.013	220.313	Pm^{147}	41.4		0.917	197.044
Ag^{109}	89		0.001	220.300	Ru^{101}	40.9	1.52	0.990	196.127
U^{236}	87		1.600	220.299	Ag^{109}	40.8		0.002	195.137
Pr^{141}	85.5	0.128	0.142	218.699	I^{127}	37.8	0.160	0.113	195.135
Cs^{133}	83.1	0.160	0.162	218.557	U^{236}	34.6		1.380	195.022
I^{127}	78.5	0.004	0.022	218.395	Pm^{147}	33.4		0.347	193.642
La^{139}	73.5	0.080	0.567	218.373	I^{127}	31.4		0.083	193.295
Ag^{109}	72.4		0.004	217.806	Ag^{109}	30.9	0.007	0.006	193.212
I^{129}	72.4		0.048	217.802	U^{236}	30.2		0.450	193.206
U^{236}	72		2.250	217.754	Eu^{153}	24.1		0.015	192.756
Mo^{97}	71.8	0.420	0.402	215.504	Ru^{101}	24.1	1.91	1.050	192.741
Rh^{103}	68		0.003	215.102	Cs^{133}	22.6	1.68	1.648	191.691
I^{127}	66.3	0.005	0.003	215.099	Eu^{153}	21.1	0.003	0.004	190.043
I^{129}	66.2		0.004	215.096	I^{127}	20.5	0.030	0.017	190.039
Ag^{109}	56.7	0.003	0.003	215.092	Eu^{153}	20.1	0.067	0.078	190.022
Nd^{143}	56.0	0.808	0.807	215.089	Pm^{147}	20.0		0.428	189.994
Pm^{147}	50.3		0.490	214.282	Eu^{153}	18.8	0.027	0.033	189.516
Cs^{133}	47.8	9.92	0.975	213.792	Eu^{153}	18.1	0.026	0.032	189.483
Pm^{147}	47.2		0.637	212.817	Eu^{153}	16.8	0.013	0.016	189.451
Rh^{103}	46.5		0.022	212.180	Eu^{153}	16.3		0.001	189.435
I^{127}	46.3	0.067	0.041	212.158	Pm^{147}	15.6		0.389	189.434

Table 6 (continued)

Fission Product	E_0 (ev)	yI_{res} (barns per fission) From (ref 18)	yI_{res} (barns per fission) This Paper	$\sum_i y_i I_{res}$ (barns per fission)	Fission Product	E_0 (ev)	yI_{res} (barns per fission) From (ref 18)	yI_{res} (barns per fission) This Paper	$\sum_i y_i I_{res}$ (barns per fission)
Ru^{101}	15.2	2.530	1.380	189.045	U^{236}	5.49		38.950	112.281
Xe^{131}	14.1	10.4*	20.150	187.665	Pm^{147}	5.43		37.021	73.331
Eu^{153}	13.3	0.003	0.003	167.515	Ag^{109}	5.20		0.391	36.310
Eu^{153}	11.7	0.066	0.080	167.512	Eu^{153}	4.81		0.008	35.919
Ru^{101}	9.8	4.320	2.430	167.432	Nd^{145}	4.37	4.94	4.786	35.911
In^{115}	9.1		0.004	165.002	Eu^{153}	3.94	0.179	0.219	31.125
Eu^{153}	8.87	0.122	0.143	164.998	In^{115}	3.86		0.005	30.906
Sm^{152}	8.1	18.200	20.950	164.855	Eu^{153}	3.29	0.130	0.281	30.901
Eu^{153}	7.6	0.010	0.009	143.905	Eu^{153}	2.46	0.730	0.645	30.620
Pm^{147}	7.00		4.114	143.896	Eu^{153}	1.76	0.060	0.061	29.975
Pm^{147}	6.64		1.623	139.782	In^{115}	1.46	0.340	0.319	29.914
Eu^{153}	6.25		0.055	138.159	Rh^{103}	1.257	23.50	29.348	29.595
Cs^{133}	5.90	19.40	19.263	138.104	Pm^{147}	1.04		0.247	0.247
Tc^{99}	5.62	1.63	6.560	118.841					

*At E_0 = 9.2.

Table 7. Excess Resonance Integral of the U^{233} and Pu^{239} Fission Product Aggregates

Fission Product	Excess Resonance Integral Below 100 ev, $I_{<100}$ (barns)	y (%)		y $I_{<100}$ (barns per fission)	
		For U^{233}	For Pu^{239}	For U^{233}	For Pu^{239}
Pm^{147}	1950	1.71	2.92	33.35	56.94
Rh^{103}	980	1.6	5.80	15.68	56.84
Cs^{133}	345.2	6.18	5.27	21.33	18.19
Xe^{131}	687.7	3.74	2.87	25.72	19.74
Sm^{152}	2850	0.43	2.00	12.26	57.00
Tc^{99}	108.2	4.8	5.9	5.18	6.37
Nd^{145}	243.5	3.00	4.24	7.31	10.32
Mo^{95}	96.4	6.1	6.27	5.88	6.04
Ru^{101}	116.8	3.00	5.0	3.50	5.84
Eu^{153}	1121	0.095	0.41	1.06	4.60
Nd^{143}	13.5	5.2	6.31	0.70	0.85
La^{139}	8.66	5.91	5.70	0.51	0.49
Ag^{109}	1358	0.04	1.50	0.41	20.37
Mo^{97}	6.60	5.35	6.09	0.35	0.40
In^{115}	3166	0.02	0.041	0.63	1.30
I^{127}	117	0.25	0.39	0.29	0.46
Pr^{141}	2.4	5.57	6.02	0.13	0.14
I^{129}	6.4	0.90	5.5×10^{-4}	0.05	0
			Total	134.34	265.89

The thermal cross section and resonance integrals for different burnups and flux conditions have been calculated by Eq. 5 for the fission product aggregates of each of the three fissionable nuclides. The results are shown in Tables 8, 9, and 10, together with the corresponding values resulting from summing over the four pseudoelements. Over the range of P,F values considered, it is seen that the pseudoelements adequately reproduce the actual fission product aggregate characteristics.

In Tables 11, 12, and 13 are listed the yields, thermal cross sections, and energy-distributed excess resonance integrals of the four pseudoelements representing the fission product aggregates of the three fuels considered. From the data here, the thermal group cross sections and the multigroup cross sections have been calculated and are listed

Table 8. Variation of the U^{233} Fission Product Aggregate Absorption Cross Section with Fractional Burnup and Flux Spectrum at a Neutron Temperature of 1000°K and a Reactor Specific Power of 2000 kw/kg

P	Calculational Method*	F = 0	F = 0.5	F = 1.0	F = 1.5	F = 2.0
		Thermal Cross Section (barns per fission)				
0	A	37.04	33.90	31.23	28.93	26.94
	B	37.04	34.23	31.74	29.56	27.60
0.1	A	37.04	33.72	30.89	28.47	26.37
	B	37.04	33.95	31.22	28.83	26.71
0.2	A	37.04	33.55	30.59	28.08	25.94
	B	37.04	33.67	30.76	28.24	26.03
0.3	A	37.04	33.41	30.37	27.79	25.63
	B	37.04	33.41	30.36	27.75	25.51
0.4	A	37.04	33.26	30.13	27.58	25.40
	B	37.04	33.18	30.02	27.36	25.08
		Excess Resonance Integral Below 100 ev (barns per fission)				
0	A	134.34	126.91	118.94	112.46	106.66
	B	134.34	128.07	122.29	116.94	111.99
0.1	A	134.34	122.38	112.37	103.74	96.72
	B	134.34	123.49	114.12	106.03	98.97
0.2	A	134.34	118.82	106.61	96.80	88.82
	B	134.34	119.27	107.20	97.41	89.33
0.3	A	134.34	115.51	101.50	90.79	82.36
	B	134.34	115.39	101.28	90.46	81.92
0.4	A	134.34	112.55	96.96	85.64	76.94
	B	134.34	111.82	96.16	84.73	76.01

*Method A: summing over the individual fission products in Table 3.
Method B: summing over the four pseudoelements in Table 11.

in Tables 14 and 15 for each of the three fission product aggregates. The non-1/v properties of the components of each pseudoelement are taken into account in computing the thermal group cross sections by determining the actual

Table 9. Variation of the U^{235} Fission Product Aggregate Absorption Cross Section with Fractional Burnup and Flux Spectrum at a Neutron Temperature of 1000°K and a Reactor Specific Power of 2000 kw/kg

(U^{236} not included in the aggregate)

P	Calculational Method*	F = 0	F = 0.5	F = 1.0	F = 1.5	F = 2.0
		Thermal Cross Section (barns per fission)				
0	A	43.00	39.23	36.02	33.27	30.90
	B	43.00	39.83	37.00	34.48	32.24
0.1	A	43.00	37.86	33.68	30.33	27.58
	B	43.00	38.26	34.32	31.02	28.22
0.2	A	43.00	36.64	31.95	28.33	25.45
	B	43.00	36.92	32.32	28.68	25.73
0.3	A	43.00	35.60	30.59	26.86	23.95
	B	43.00	35.77	30.74	26.96	23.94
0.4	A	43.00	34.72	29.49	25.73	22.81
	B	43.00	34.77	29.47	25.59	22.56
		Excess Resonance Integral Below 100 ev (barns per fission)				
0	A	172.40	161.11	151.41	142.65	134.82
	B	172.40	164.21	156.63	149.63	143.13
0.1	A	172.40	145.38	125.70	110.95	99.54
	B	172.40	146.76	127.55	112.76	101.13
0.2	A	172.40	131.64	107.24	91.07	79.54
	B	172.40	132.86	108.32	91.85	80.07
0.3	A	172.40	121.62	95.03	78.79	67.74
	B	172.40	121.59	94.76	78.55	67.13
0.4	A	172.40	112.71	85.27	69.47	59.02
	B	172.40	112.28	84.68	68.71	58.14

*Method A: summing over the individual fission products listed in Table 3.

Method B: summing over the four pseudoelements in Table 12.

$$\sum_{i}^{gr} y_i \, g_i(T) \, \sigma_{io}$$

for each pseudoelement and normalizing the result to the pseudoelement yield.

Table 10. Variation of the Pu^{239} Fission Product Aggregate Absorption Cross Section with Fractional Burnup and Flux Spectrum at a Neutron Temperature of 1000°K and a Reactor Specific Power of 2000 kw/kg

P	Calculational Method*	F = 0	F = 0.5	F = 1.0	F = 1.5	F = 2.0
		Thermal Cross Section (barns per fission)				
0	A	53.74	52.18	50.70	49.31	47.96
	B	53.74	52.56	51.41	50.28	49.21
0.1	A	53.74	49.51	45.95	42.88	40.26
	B	53.74	49.65	46.18	43.19	40.57
0.2	A	53.74	47.19	42.34	38.58	35.52
	B	53.74	47.20	42.28	38.45	35.34
0.3	A	53.74	45.20	39.55	35.73	32.24
	B	53.74	45.05	39.24	35.00	31.72
0.4	A	53.74	43.49	37.29	32.98	29.77
	B	53.74	43.19	36.78	32.35	28.99
		Excess Resonance Integral Below 100 ev (barns per fission)				
0	A	265.89	256.80	248.41	240.66	233.49
	B	265.89	261.14	256.50	251.98	247.61
0.1	A	265.89	229.32	201.17	179.09	161.41
	B	265.89	231.57	204.32	182.42	164.55
0.2	A	265.89	206.87	168.82	142.73	123.92
	B	265.89	207.60	169.21	142.66	123.48
0.3	A	265.89	188.36	145.57	119.10	101.19
	B	265.89	187.93	144.47	117.63	99.59
0.4	A	265.89	172.90	128.18	102.50	85.83
	B	265.89	171.61	126.30	100.54	83.96

*Method A: summing over the individual fission products listed in Table 3.
Method B: summing over the four pseudoelements in Table 13.

Table 11. Yields, Thermal Cross Sections, and Energy-Distributed Excess Resonance Integrals of the Pseudoelements Representing the Fission Product Aggregates of U^{233}

Pseudoelement No. 1		Pseudoelement No. 2				Pseudoelement No. 3	
$y = 9.43\%$		$y = 18.1\%$				$y = 5.13\%$	
$g\sigma_0 = 228.31$ barns		$g\sigma_0 = 30.88$ barns				$g\sigma_0 = 147.56$ barns	
$I_T = 113.89$ barns		$I_T = 284.48$ barns				$I_T = 836.25$ barns	
E_0 (ev)	I_{res} (barns)	E_0 (ev)	I_{res} (barns)	E_0 (ev)	I_{res} (barns)	E_0 (ev)	I_{res} (barns)
		4.37	20.083	40.9	3.282		
56	7.423	5.62	28.619	43.1	20.276	1.257	305.107
66.2	0.042	5.90	99.801	45.0	32.486	14.1	501.365
71.8	3.712	9.80	8.055	46.3	0.227	46.5	0.235
72.4	0.509	15.2	4.575	47.8	5.055	68.0	0.040
73.5	5.408	20.5	0.094	66.3	0.017	95.0	0.273
85.5	1.379	22.6	8.536	78.5	0.116	100.0	0
95.6	0.021	24.1	3.481	83.1	0.840		
100	0	31.4	0.459	91.0	0.066		807.020
		37.8	0.624	94.8	1.260		
	18.494			100	2.328		
					240.280		

Pseudoelement No. 4							
$y = 1.75\%$		$g\sigma_0 = 134.29$ barns		$I_T = 2812.0$ barns			
1.04	10.571	6.25	2.000	16.3	0	40.8	0.114
1.46	34.971	6.64	66.571	16.8	0.571	41.4	37.657
1.76	2.229	7.00	168.800	18.1	1.143	43.2	7.714
2.46	23.314	7.60	0.286	18.8	1.200	47.2	26.171
3.29	10.171	8.10	700.571	20.0	17.543	50.3	20.114
3.86	0.571	8.87	5.143	20.1	2.800	56.7	0.171
3.94	7.943	9.10	0.457	21.1	0.171	72.4	0.229
4.81	0.286	11.7	2.857	24.1	0.571	89.0	0.057
5.20	22.514	13.3	0.114	30.9	0.343	100	0
5.43	1519.943	15.6	15.943	33.4	14.286		
							2726.11

Table 12. Yields, Thermal Cross Sections, and Energy-Distributed Excess Resonance Integrals of the Pseudoelements Representing the Fission Product Aggregates of U^{235}

Pseudoelement No. 1		Pseudoelement No. 2				Pseudoelement No. 3	
$y = 11.24\%$		$y = 21.0\%$				$y = 5.82\%$	
$g\sigma_0 = 216.81$ barns		$g\sigma_0 = 31.52$ barns				$g\sigma_0 = 140.94$ barns	
$I_T = 71.0$ barns		$I_T = 283.1$ barns				$I_T = 905.54$ barns	
E_0 (ev)	I_{res} (barns)	E_0 (ev)	I_{res} (barns)	E_0 (ev)	I_{res} (barns)	E_0 (ev)	I_{res} (barns)
		4.37	22.790	40.9	4.714		
56	7.206	5.62	31.238	43.1	23.010	1.257	504.261
66.2	0.039	5.90	91.729	45.0	28.781	14.1	346.220
71.8	3.559	9.80	11.571	46.3	0.195	46.5	0.378
72.4	0.472	15.2	6.571	47.8	4.643	68.0	0.052
73.5	5.071	20.5	0.081	66.3	0.014	95.0	0.464
85.5	1.246	22.6	7.848	78.5	0.105	100.0	0
95.6	0.027	24.1	5.00	83.1	0.771		
100	0	31.4	0.395	91.0	0.752		851.375
		37.8	0.538	94.8	1.157		
	17.62			100	1.427		
					243.33		

Pseudoelement No. 4							
$y = 2.95\%$		$g\sigma_0 = 129.15$ barns		$I_T = 2449.83$ barns			
1.04	8.373	6.25	1.865	16.3	0.034	40.8	0.067
1.46	10.813	6.64	55.017	16.8	0.543	41.4	31.08
1.76	2.068	7.00	139.457	18.1	1.085	43.2	6.339
2.46	21.865	7.60	0.305	18.8	1.119	47.2	21.593
3.29	9.525	8.1	710.169	20.0	14.508	50.3	16.610
3.86	0.170	8.87	4.847	20.1	2.644	56.7	0.102
3.94	7.424	9.10	0.136	21.1	0.136	72.4	0.170
4.81	0.271	11.7	2.712	24.1	0.509	89.0	0.067
5.20	13.254	13.3	0.102	30.9	0.203		0
5.43	1254.949	15.6	13.186	33.4	11.763	100	
							2365.08

Table 13. Yields, Thermal Cross Sections, and Energy-Distributed Excess Resonance Integrals of the Pseudoelements Representing the Fission Product Aggregates of Pu^{239}

Pseudoelement No. 1 $y = 11.7\%$ $g\sigma_0 = 204.70$ barns $I_T = 90.86$ barns		Pseudoelement No. 2 $y = 20.27\%$ $g\sigma_0 = 31.52$ barns $I_T = 277.4$ barns				Pseudoelement No. 3 $y = 8.6\%$ $g\sigma_0 = 169.65$ barns $I_T = 918.38$ barns	
E_0 (ev)	I_{res} (barns)	E_0 (ev)	I_{res} (barns)	E_0 (ev)	I_{res} (barns)	E_0 (ev)	I_{res} (barns)
		4.37	25.442	40.9	4.884		
56	7.265	5.62	31.426	43.1	25.585	1.257	659.757
66.2	0	5.90	75.994	45.0	29.817	14.1	229.536
71.8	3.419	9.80	11.988	46.3	0.321	46.5	0.489
72.4	0	15.2	6.808	47.8	3.848	68.0	0.071
73.5	4.188	20.5	0.138	66.3	0.030	95.0	0.617
85.5	1.198	22.6	6.502	78.5	0.168	100	0
95.0	0	24.1	5.180	83.1	0.641		
100		31.4	0.641	91.0	0.099		890.47
	16.070	37.8	0.873	94.8	0.957		
				100	1.658		
					233.000		

Pseudoelement No. 4

$y = 6\%$ $g\sigma_0 = 146.83$ barns $I_{res} = 2399.33$ barns

1.04	5.183	6.25	2.500	16.3	0.100	40.8	1.800
1.46	21.000	6.64	33.150	16.8	0.750	41.4	18.767
1.76	2.800	7.00	84.083	18.1	1.433	43.2	3.833
2.46	29.367	7.60	0.383	18.8	1.483	47.2	13.033
3.29	12.783	8.10	950.000	20.0	8.750	50.3	10.133
3.86	0.333	8.87	6.500	20.1	3.533	56.7	2.417
3.94	10.000	9.10	0.333	21.1	0.183	72.4	3.483
4.81	0.367	11.70	3.633	24.1	0.700	89.0	0.567
5.20	326.033	13.3	0.150	30.9	5.200	100	0
5.43	757.00	15.6	7.950	33.4	7.117		
							2336.83

Table 14. Thermal Group Cross Sections for U^{233}, U^{235}, and Pu^{239} Fission Product Pseudoelements

$$\bar{\sigma}_{TH} = \left(\frac{\pi T_0}{4T}\right)^{1/2} g\sigma_0$$

Fuel	Group	Lethargy	Temperature (°F)	Energy (ev)	$\bar{\sigma}_{TH}$ (barns)			
					Pseudo-element No. 1	Pseudo-element No. 2	Pseudo-element No. 3	Pseudo-element No. 4
U^{233}	23	18.0	2704	0.1523	82.737	11.774	73.228	48.712
	24	18.2	2145	0.1247	91.011	12.968	67.619	53.832
	25	18.4	1673	0.1021	100.44	14.283	67.937	59.242
	26	18.6	1286	0.08358	111.63	15.705	71.379	65.196
	27	18.8	970	0.06843	124.46	17.297	77.102	72.979
	28	19.0	711	0.05603	138.49	19.083	83.698	81.331
	29	19.2	499	0.04587	153.62	20.981	91.733	90.263
	30	19.4	325	0.03756	170.38	23.026	100.67	100.58
	31	19.6	185	0.03075	188.48	25.359	110.63	112.54
	32	19.8	69	0.02530	208.26	27.909	121.45	124.58
U^{235}	23	18	2704	0.1523	75.359	12.126	76.338	44.202
	24	18.2	2145	0.1247	82.393	13.306	73.320	48.714
	25	18.4	1673	0.1021	91.058	14.600	73.678	53.687
	26	18.6	1286	0.08358	101.25	16.067	76.991	59.171
	27	18.8	970	0.06843	112.90	17.731	81.756	65.760
	28	19.0	711	0.05603	125.67	19.567	88.407	72.876
	29	19.2	499	0.04587	139.54	21.532	96.124	81.212
	30	19.4	325	0.03756	154.66	23.656	104.98	90.734
	31	19.6	185	0.03075	171.28	26.030	114.92	100.82
	32	19.8	69	0.02530	189.23	28.528	126.39	112.06

Table 14 (continued)

Fuel	Group	Lethargy	Temperature (°F)	Energy (ev)	$\bar{\sigma}_{TH}$ (barns)			
					Pseudo-element No. 1	Pseudo-element No. 2	Pseudo-element No. 3	Pseudo-element No. 4
Pu^{239}	23	18	2704	0.1523	74.403	12.260	84.002	53.579
	24	18.2	2145	0.1247	81.610	13.391	80.486	59.145
	25	18.4	1673	0.1021	90.118	14.691	79.516	65.071
	26	18.6	1286	0.08358	100.10	16.116	81.754	71.837
	27	18.8	970	0.06843	111.55	17.759	86.595	79.932
	28	19.0	711	0.05603	124.30	19.479	92.790	88.832
	29	19.2	499	0.04587	138.16	21.463	100.26	98.726
	30	19.4	325	0.03756	153.24	23.683	109.19	110.31
	31	19.6	185	0.03075	169.70	26.095	119.55	123.79
	32	19.8	69	0.02530	187.40	28.637	130.87	137.66

Table 15. Group Cross Sections for U^{233}, U^{235}, and Pu^{239} Fission Product Pseudoelements

$$\bar{\sigma} = \frac{\int_{E_1}^{E_2} \sigma(E) \frac{dE}{E}}{\int_{E_1}^{E_2} \frac{dE}{E}}$$

Group	Energy Limits (ev)	ΔU	U^{233} $\bar{\sigma}$ (barns)				U^{235} $\bar{\sigma}$ (barns)				Pu^{239} $\bar{\sigma}$ (barns)			
			Pseudo-element No. 1	Pseudo-element No. 2	Pseudo-element No. 3	Pseudo-element No. 4	Pseudo-element No. 1	Pseudo-element No. 2	Pseudo-element No. 3	Pseudo-element No. 4	Pseudo-element No. 1	Pseudo-element No. 2	Pseudo-element No. 3	Pseudo-element No. 4
1	10^7–6.065×10^6	0.5	0.013	0.0017	0.0084	0.0077	0.012	0.002	0.008	0.007	0.0117	0.0018	0.0097	0.0084
2	6.065×10^6	0.5	0.018	0.0024	0.011	0.0104	0.017	0.002	0.011	0.010	0.0158	0.0024	0.0131	0.0114
3	3.679×10^6	0.5	0.022	0.0029	0.014	0.0127	0.020	0.003	0.013	0.012	0.0193	0.0030	0.0160	0.0138
4	2.231×10^6	0.5	0.028	0.0037	0.018	0.0162	0.026	0.004	0.017	0.016	0.0248	0.0038	0.0205	0.0178
5	1.353×10^6	0.5	0.035	0.0048	0.023	0.021	0.034	0.005	0.022	0.020	0.0318	0.0049	0.0264	0.0228
6	8.208×10^5	0.5	0.606	0.266	0.201	0.529	0.363	0.236	0.339	0.432	0.4788	0.2663	0.1978	0.3953
7	4.98×10^5	0.5	0.718	0.314	0.240	0.626	0.430	0.286	0.414	0.643	0.5684	0.3141	0.2354	0.4696
8	3.02×10^5	0.5	0.851	0.370	0.287	0.742	0.499	0.336	0.492	0.720	0.6753	0.3724	0.2838	0.5563
9	1.832×10^5	3.0	1.719	0.732	0.593	1.483	1.038	0.662	0.987	1.467	1.3696	0.7352	0.5914	1.1237
10	9.118×10^3	3.0	9.979	4.332	3.357	8.687	5.927	3.912	5.705	8.578	7.9194	4.3538	3.3159	6.5247
11	4.54×10^2	1.4	41.837	18.567	13.652	36.803	24.363	16.742	23.848	36.362	33.064	18.666	13.347	27.368
12	112	1.2	26.299	58.998	5.401	85.208	22.626	58.330	7.170	71.544	22.482	60.944	6.2943	52.126
13	33.72	0.8	7.689	22.471	4.970	72.774	7.302	25.931	4.747	61.513	6.8943	25.148	5.7138	51.519
14	15.15	0.4	10.327	1.397	1260.09	13.503	9.807	1.426	871.925	12.877	9.2594	1.4258	581.51	16.100
15	10.16	0.8	14.010	172.489	9.055	3116.45	13.305	170.107	8.649	2733.3	12.561	151.19	10.411	2709.5
16	4.564	1.2	23.294	19.887	15.056	79.701	22.121	22.208	14.380	56.398	20.886	24.418	17.309	78.550
17	1.375	0.4	34.290	4.638	784.93	46.597	32.563	4.734	1281.8	40.330	30.744	4.734	1674.9	35.010
18	0.9214	0.4	41.881	5.665	27.068	24.634	39.772	5.782	25.854	23.691	37.550	5.782	31.121	26.934
19	0.6176	0.4	51.155	6.919	33.062	30.089	48.578	7.062	31.579	28.937	45.865	7.062	38.012	32.899
20	0.4140	0.2	62.479	8.451	40.381	36.750	59.332	8.626	38.570	35.343	56.018	8.626	46.426	40.181
21	0.2775	0.2	72.498	9.806	46.856	42.642	68.846	10.009	44.754	41.010	65.000	10.009	53.871	46.624
22	0.2272	0.2	80.135	10.839	51.792	47.134	76.098	11.063	49.469	45.330	71.848	11.063	59.545	51.536
23	0.1860	0.2	88.552	11.977	57.233	52.086	84.092	12.225	54.665	50.092	79.395	12.225	65.800	56.949
24	0.1523	0.2	97.865	13.237	63.252	57.563	92.936	13.511	60.414	55.360	87.745	13.511	72.720	62.939
25	0.1247	0.2	108.16	14.628	69.902	63.616	102.71	14.932	66.766	61.181	96.970	14.932	80.367	69.556
26	0.1021	0.2	119.55	16.169	77.264	70.316	113.52	16.504	73.798	67.624	107.18	16.504	88.830	76.882
27	0.08358	0.2	132.06	17.862	85.355	77.679	125.41	18.232	81.525	74.706	118.41	18.232	97.132	84.932
28	0.06843	0.2	146.07	19.757	94.409	85.919	138.72	20.166	90.173	82.630	130.97	20.166	104.54	93.942
29	0.05603	0.2	161.35	21.823	104.28	94.903	153.22	22.275	99.602	91.270	144.66	22.275	119.89	103.76
30	0.04587	0.2	178.34	24.122	115.27	104.90	169.36	24.621	110.094	100.88	159.90	24.622	132.52	114.69
31	0.03756	0.2	197.06	26.653	127.36	115.91	187.14	27.206	121.650	111.47	176.68	27.206	146.43	126.73
32	0.03756–0.02518	0.2	217.73	29.449	140.72	128.07	206.77	30.060	134.410	123.12	195.22	30.060	161.79	140.03

Appendix 1

REACTOR SPECTRA AND EFFECTIVE CROSS SECTIONS

For reactor spectra which approximate a Maxwellian (T in °K) plus a dE/E flux terminated at the low energy end, we can represent the flux by:

$$f(E)\,dE = (n\bar{v})_M \left[\frac{E}{(KT)^2}\, e^{-E/KT} + \frac{\beta\Delta}{E}\right] dE \quad , \tag{A.1}$$

where

$$\Delta = 0 \text{ if } E < \mu KT \ ,$$

$$\Delta = 1 \text{ if } E \geqslant \mu KT \ ,$$

and the subscript M refers to the Maxwellian distribution.

Westcott (22) has defined an effective cross section $\hat{\sigma}$ as that cross section which when multiplied by the "2200 m/sec flux" gives the true reaction rate. Thus, for a nuclide with cross section $\sigma(E)$, we have as the definitive equation for the effective cross section

$$(n_M + n_{1/E})\, v_0\sigma = (nv)_M \int_0^\infty \sigma(E)\, \frac{E}{(KT)^2}\, e^{-E/KT}\, dE + $$

$$+ (n\bar{v})_M\, \beta \int_{\mu KT}^\infty \sigma(E)\, \frac{dE}{E} \quad . \tag{A.2}$$

By definition

$$(n\bar{v})_M \int_0^\infty \sigma(E)\, \frac{E}{(KT)^2}\, e^{-E/KT}\, dE = (n\bar{v})_M \int_0^\infty g\sigma_0 \left(\frac{E_0}{E}\right)^{1/2} \frac{E}{(KT)^2}\, e^{-E/KT}\, dE$$

$$= (n\bar{v})_M\, g\sigma_0 \left(\frac{\pi T_0}{4T}\right)^{1/2} \quad ,$$

$$(n\bar{v})_M\, \beta \int_{\mu KT}^\infty \sigma(E)\, \frac{dE}{E} = (n\bar{v})_M\, \beta\, \Sigma_\mu \quad .$$

From Eq. A.2, these definitions lead to Westcott's definition of $\hat{\sigma}$ as

$$\hat{\sigma} = \frac{(n\bar{v})_M}{(n_M + n_{1/E})v_0}\,\sigma_0\left[g\left(\frac{\pi T_0}{4T}\right)^{1/2} + \beta\,\frac{\Sigma_\mu}{\sigma_0}\right]$$

$$= \sigma_0\left[\frac{g + \beta\left(\frac{4T}{\pi T_0}\right)^{1/2}\frac{\Sigma_\mu}{\sigma_0}}{1 + \frac{4}{(\pi\mu)^{1/2}}\,\beta}\right]$$

$$= \sigma_0(g + rs) \quad , \qquad \text{(A.3)}$$

where

$$g = \frac{\int_0^\infty \sigma(v)\ v\ n(v)\ dv}{\sigma_0\ v_0 \int_0^\infty n(v)\ dv} \quad ,$$

$$r = \frac{\beta}{1 + \frac{4}{(\pi\mu)^{1/2}}\,\beta} \quad ,$$

$$s = \left(\frac{4T}{\pi T_0}\right)^{1/2}\frac{\Sigma_\mu}{\sigma_0} - bg \quad .$$

Appendix 2

CALCULATION OF THE RESONANCE ABSORPTION INTEGRAL

When there are separate neutron resonances, the contribution of each resonance to the total resonance integral can be computed if the resonance parameters are known. This is accomplished by integrating over the Breit-Wigner single resonance formula for l = 0 interactions. The restriction to zero orbital angular momentum is not serious, since these resonances constitute nearly all the contributions to the total resonance integral. The Breit-Wigner single level formula is:

$$\sigma_{n,\gamma}(E) = \frac{\pi \lambda\!\!\!^{-2} g\, \Gamma_n(E)\, \Gamma_\gamma}{(E - E_0)^2 + \left(\frac{\Gamma}{2}\right)^2} \tag{A.4}$$

in which

$$\lambda\!\!\!^{-2} = \lambda\!\!\!^{-2}_0 \frac{E_0}{E}$$

$$\Gamma_n(E) = \Gamma_n \left(\frac{E_0}{E}\right)^{1/2}$$

$$g = \frac{1}{2}\left(1 \pm \frac{1}{2I + 1}\right) ,$$

and the symbols are defined as follows:

$\lambda\!\!\!^{-}$ = the reduced de Broglie wave length for neutrons of energy E,

E_0 = the resonance energy,

Γ_n = the neutron width at resonance energy,

g = the statistical weight factor where I is the spin of the target nucleus,

$\Gamma = \Gamma_n + \Gamma_\gamma$.

Expressing Eq. A.4 in terms of the parameters at E_0 yields

$$\sigma_{n,\gamma}(E) = \pi\lambda\!\!\!^{-}{}_0^2 \left(\frac{E_0}{E}\right)^{1/2} \frac{g\Gamma_n\Gamma_\gamma}{(E - E_0)^2 + \left(\frac{\Gamma}{2}\right)^2} \quad . \tag{A.5}$$

It is desired to find the contribution of the peak alone to

$$\int_{total} \sigma(E) \frac{dE}{E} \quad ,$$

where the total resonance integral contains a 1/v contribution, as well as contributions from the peaks. If the resonance peak is narrow, then E is nearly the constant E_0 in the region where the maximum part of the peak resonance integral is generated:

$$I_T = \int_{peak} \sigma(E) \frac{dE}{E} = \pi\lambda\!\!\!^{-}{}_0^2 \left(\frac{E_0}{E_0}\right)^{1/2} g\Gamma_n\Gamma_\gamma \int_0^\infty \frac{dE}{\left[(E - E_0)^2 + \left(\frac{\Gamma}{2}\right)^2\right] E_0}$$

$$= 2\pi^2\lambda\!\!\!^{-}{}_0^2 \frac{g\Gamma_n\Gamma_\gamma}{\Gamma E_0} \quad . \tag{A.6}$$

This expression gives the peak or excess over 1/v contribution of a given resonance to the total resonance integral. Putting in the values of the basic physical constants it becomes, in barns,

$$I_{res} = \frac{4.09 \times 10^6}{E_0^2} \frac{g\Gamma_n\Gamma_\gamma}{\Gamma} \quad . \tag{A.7}$$

Because of the difficulty associated with obtaining experimental data for high energy resonances, both the resonance parameters and the resonance energy are often unknown above a certain energy E_1. It is necessary to make an estimate based on the systematics of neutron resonance parameters. If D is the average spacing of levels and $\overline{\Gamma}_0$ and $\overline{\Gamma}_n^0$ are the local widths averaged over several resonances, then according to Dresner (23), the average contribution to the resonance integral

above an energy E_1 to infinity is

$$I_{res} = 1.3 \times 10^6 \frac{\pi g \overline{\Gamma}_\gamma}{D} \int_{E_1}^{\infty} \frac{dE}{\left(1 + \frac{\overline{\Gamma}_\gamma}{\Gamma_n}\right) t}$$

$$= \frac{1.3 \times 10^6}{E_1} \frac{2\pi g \overline{\Gamma}_\gamma}{D} \frac{\beta - \ln(1 + \beta)}{\beta^2} , \qquad (A.8)$$

where

$$\beta = E^{-1/2} \frac{\overline{\Gamma}_\gamma}{\overline{\Gamma}^0_n} .$$

The above expression, as originally developed by Dresner, is based on the assumption that the reduced neutron width is a constant for all resonances. Kuhn and Dresner (24) have more recently calculated a correction factor to bring Eq. A.8 into agreement with the Porter-Thomas distribution in which it is assumed that the reduced neutron widths are distributed in a X-squared distribution with one degree of freedom. Equation A.8, together with the correction factor, were used in this study in all estimates of the resonance integral for higher energies.

References

1. A. M. Weinberg and E. P. Wigner, The Physical Theory of Neutron Chain Reactors, The University of Chicago Press, Chicago, 1958.

2. J. B. Sampson et al., Poisoning in Thermal Reactors Due to Stable Fission Products, KAPL-1226 (Oct. 4, 1954).

3. C. H. Westcott, Effective Cross Section Values for Well-Moderated Thermal Reactor Spectra, CRRP-787, 1958 Revision (Aug. 1, 1958).

4. S. Katcoff, Fission Product Yields from U, Th and Pu, Nucleonics 4, 78 (1958).

5. D. J. Hughes and R. B. Schwartz, Neutron Cross Sections, 2nd Ed., BNL-325 (July 1, 1958).

6. N. J. Pattenden, Fission Product Poisoning Data, ORNL-2778 (July 29, 1959).

7. T. A. Eastwood et al., Radiochemical Methods Applied to the Determination of Cross Sections of Reactor Interest, A/Conf.15/P/203.

8. J. A. Harvey et al., Low Energy Neutron Cross Sections of Radioactive Fission Product Nuclides, A/Conf.15/P/673.

9. R. L. Macklin and H. S. Pomerance, Resonance Capture Integrals, Progress in Nuclear Energy, Series I, p 179, McGraw-Hill, New York, 1956.

10. S. P. Harris et al., Phys. Rev. 79 (1), 11 (1950).

11. V. L. Sailor, Phys. Rev. 91 (1), 53 (1953).

12. H. Rose et al., The Use of the Pile Oscillator in Thermal Reactor Problems, A/Conf.15/P/14.

13. D. R. Bidinosti et al., Mass-Spectrometric Studies of Pile Poisons and Their Yields in the Fission of U^{233}, U^{235} and Pu^{239}, A/Conf.15/P/201.

14. R. B. Tattersall et al., Pile Oscillator Measurements of Resonance Absorption Integrals, AERE-R/2887 (Aug. 1959).

15. V. M. Gryazev, Atomnaya Energiya 3, 507-14 (1957).

16. P. Greebler, H. Hurwitz, Jr., and M. L. Storm, Statistical Evaluation of Fission Product Absorption Cross Sections at Intermediate and High Energies, Nuc. Sci. Eng. 2, 334-351 (1957).

17. U. L. Busenaro, S. Gallone, and D. Morgan, Monte Faito Conference of European Nuclear Society (1956).

18. I. V. Gordeev and V. Ya. Pupko, Evaluation of the Absorption Cross Section of U^{235} Fission Fragments in the 0.025–10^6 ev Energy Range and Calculation of Fragment Effects in Intermediate Reactors, A/Conf.15/P/2223.

19. N. J. Pattenden, Some Neutron Cross Sections of Importance to Reactors Tc^{99}, Nd^{143}, Nd^{145}, Sm^{149}, Sm^{152}, Eu^{151}, Eu^{153}, Gd^{155}, Gd^{157} and Pu^{240}, A/Conf.15/P/11.

20. C. H. Westcott and D. A. Roy, Supplement to Effective Cross Section Values for Well-Moderated Thermal Reactor Spectra, CRRP-862 (Aug. 20, 1959).

21. Reactor Physics Constants, ANL-5800, Argonne National Laboratory.

22. C. H. Westcott, The Specification of Neutron Flux and Effective Cross Sections in Reactor Calculations, CRRP-662 (Aug. 15, 1956).

23. L. Dresner, J. Nuc. Energy 2, 118 (1955).

24. E. Kuhn and L. Dresner, J. Nuc. Energy 7, 69 (1958).

Bibliography

1. Blomeke, J. O. and Mary F. Todd, U^{235} Fission Product Production as a Function of Thermal Neutron Flux, Irradiation Time, and Decay Time: I. Atomic Concentrations and Gross Totals, ORNL-2127, Part 1, Vol. 1 (Aug. 19, 1957).

2. Craig, D. S., et al., Long Irradiation of Natural Uranium, A/Conf.15/P/205.

3. Hughes, D. J., Neutron Cross Sections, Pergamon Press, New York, 1957.

4. Hughes, D. J., and R. L. Zimmerman, Systematics of Neutron Resonance Parameters, A/Conf.15/P/1036.

5. Hurst, D. G., J. M. Kennedy, and W. H. Walker, Cross Sections and Yields of Pseudo-Fission-Products, CRRP-760, AECL No. 715 (Oct. 27, 1958).

6. Webster, J. W., The Low Cross Section Fission Product Poisons, IDO-16100 (June 8, 1953).

7. Westcott, C. H., Effective Cross Section Values for Well-Moderated Thermal Reactor Spectra, CRRP-680, TNCC(CAN)-7 (Jan. 25, 1957).

ORNL-2869

Reactors—Power
TID-4500 (15th ed.)

INTERNAL DISTRIBUTION

1. L. G. Alexander
2. D. S. Billington
3. E. P. Blizard
4. A. L. Boch
5. C. J. Borkowski
6. G. E. Boyd
7. R. B. Briggs
8. A. D. Callihan
9. R. S. Carlsmith
10. C. E. Center (K-25)
11. R. A. Charpie
12. R. R. Coveyou
13. F. L. Culler
14. T. K. DeBoer
15. J. G. Delene
16. L. Dresner
17. L. B. Emlet (K-25)
18. A. P. Fraas
19. J. H. Frye
20. D. R. Gilfillan
21. W. R. Grimes
22. E. E. Gross
23. E. Guth
24. W. Hafele
25. C. S. Harrill
26. A. Hollaender
27. A. S. Householder
28. S. Jaye
29. W. H. Jordan
30. P. R. Kasten
31 C. P. Keim
32. M. T. Kelley
33. W. E. Kinney
34. P. G. Lafyatis
35. J. A. Lane
36. R. S. Livingston
37. H. G. MacPherson
38. F. C. Maienschein
39. W. D. Manly
40. H. C. McCurdy
41. J. R. McNally
42. K. Z. Morgan
43. J. P. Murray (Y-12)
44. F. H. Neill
45. M. L. Nelson
46. E. A. Nephew
47. C. W. Nestor, Jr.
48. N. J. Pattenden
49. A. M. Perry
50. P. H. Pitkanen
51. C. A. Preskitt
52. P. M. Reyling
53. T. H. Row
54. H. W. Savage
55. A. W. Savolainen
56. H. E. Seagren
57. E. D. Shipley
58. A. Simon
59. M. J. Skinner
60. A. H. Snell
61. J. A. Swartout
62. E. H. Taylor
63. A. M. Weinberg
64. C. E. Winters
65-144. Laboratory Records Department
145. Laboratory Records, ORNL R.C.
146. Biology Library
147-148. Central Research Library
149. Health Physics Library
150-152. ORNL – Y-12 Technical Library Document Reference Section
153. Reactor Experimental Engineering Library

EXTERNAL DISTRIBUTION

154. E. R. Cohen, Atomics International
155. M. C. Edlund, Babcock & Wilcox
156. P. Greebler, General Electric, San Jose
157. L. Nordheim, General Atomic
158. B. Wolfe, General Electric, San Jose
159. P. M. Wood, Allis-Chalmers Mfg. Co.
160. Division of Research and Development, AEC, ORO
161-737. Given distribution as shown in TID-4500 (15th ed.) under Reactors—Power category (75 copies - OTS)